COLLAGEN-BASED SCAFFOLDS FOR CORNEA TISSUE ENGINEERING

A THESIS SUBMITTED TO
THE GRADUATE SCHOOL OF NATURAL AND APPLIED SCIENCES
OF
MIDDLE EAST TECHNICAL UNIVERSITY

BY

NİHAL ENGİN VRANA

IN PARTIAL FULFILLMENT OF THE REQUIREMENTS
FOR
THE DEGREE OF MASTER OF SCIENCE
IN
BIOTECHNOLOGY

SEPTEMBER 2006

Approval of the Graduate School of Natural and Applied Sciences

Prof. Dr. Canan Özgen
Director

I certify that this thesis satisfies all the requirements as a thesis for the degree of Master of Science.

Prof. Dr. Fatih Yıldız
Head of Department

This is to certify that we have read this thesis and that in our opinion it is fully adequate, in scope and quality, as a thesis and for the degree of Master of Science.

Dr. David Stuart Hulmes
Co-Supervisor

Prof. Dr. Vasıf Hasırcı
Supervisor

Examining Committee Members

Prof. Dr. Meral Yücel (METU, BIOL)

Prof. Dr. Vasıf Hasırcı (METU, BIOL)

Prof. Dr. Mesude İşcan (METU, BIOL)

Prof. Dr. Kuyaş Buğra (BOUN, MOLGEN)

Assist. Prof. Ayşe Elif Erson (METU, BIOL)

I hereby declare that all information in this document has been obtained and presented in accordance with academic rules and ethical conduct. I also declare that, as required by these rules and conduct, I have fully cited and referenced all material and results that are not original to this work.

Name, Last name : Nihal Engin Vrana

Signature :

ABSTRACT

COLLAGEN-BASED SCAFFOLDS FOR CORNEA TISSUE ENGINEERING

Vrana, Nihal Engin
M.S., Department of Biotechnology
Supervisor : Prof. Dr. Vasıf Hasırcı
Co-Supervisor : Dr. David Stuart Hulmes

September 2006, 87 pages

In this study, collagen based scaffolds were prepared for cornea tissue engineering. Three different cell carriers (rat tail collagen foam, insoluble collagen foam and patterned collagen film) were produced using two different collagen sources. Scaffolds were designed to mimic the unique topographical features of the corneal stroma. A novel crosslinking method was developed to achieve constant foam thickness. All scaffolds were tested with the primary cells of the native corneal stroma, human keratocytes. Although both foams promoted cell growth and penetration, rat tail foams were found to be superior for keratocyte proliferation. Their degradation rates were high enough but did not compromise their structural integrity during testing. Transparency studies with the foams revealed a progressive improvement. Collagen films degraded significantly over a one month period; however, the presence of cells increased the tensile strength of the films over a 21 day period to close to that of the native cornea and compensated for the loss of strength due to degradation. The micropatterned films proved to have higher transparency than the unpatterned scaffolds. In this study, it was possible to prepare collagen based micropatterned scaffolds using a silicon wafer and then a silicone template, successively, starting from original designs. The resultant collagen films were able to control cell growth through contact guidance, restricted cells and secreted-ECM within the pattern grooves, resulting in a higher transparency in comparison to unpatterned

films. Thus, the tissue engineered constructs revealed a significant potential for use as total artificial corneal substitutes.

Keywords: Tissue Engineering, Cornea, Micropatterning, Collagen, Contact guidance

Öz

KORNEA MÜHENDİSLİĞİ İÇİN KOLLAJEN TEMELLİ DOKU MÜHENDİSLİĞİ İSKELELERİ

Vrana, Nihal Engin
Yüksek Lisans, Biyoteknoloji ABD
Tez Yöneticisi : Prof. Dr. Vasıf Hasırcı
Ortak Tez Yöneticisi : Dr. David Stuart Hulmes

Eylül 2006, 87 sayfa

Bu çalışmada iki farklı kollajen kaynağı kullanılarak farklı kollajen temelli hücre iskeleleri (taşıyıcıları) (fare kuyruğu kollajen köpükler, çözünmeyen kollajen köpükler ve mikrodesenli kollajen filmler), doku mühendisliği metodlarıyla yapay kornea stroması geliştirilmesi amacıyla üretilmiştir. Bu hücre taşıyıcılarının karakterizasyonları yapılmış ve hepsi kornea stromasında bulunan keratositlerle, *in vitro* koşullarda denenmiştir. Söz konusu hücre taşıyıcıları, korneal stroma yapısı ve stromanın doğal yüzey özellikleri gözönüne alınarak tasarlanmışlardır. Fare kuyruğu kollajeni köpüklerinin sabit bir kalınlıkta üretilmesi için yeni bir çapraz bağlama metodu geliştirilmiştir. Her iki köpük tipi de hücre büyümesini ve yayılımını sağlamıştır, ancak köpüklerin farklı bozunma hızları ve fiziksel yapılarındaki farklılıklar keratositlerin farklı büyüme davranışları göstermesini sağlamıştır. Fare kuyruğu kollajeni köpüklerinin hücre büyümesi açısından daha üstün oldukları saptanmıştır. Her iki yapıda da ışık geçirgenliği gelişmesi yavaş olmaktadır. Mikrodesenli kollajen filmler, yönelimli stroma yapısının taklit edilmesinin sağlayacağı avantajları belirlemek amacıyla kullanılmıştır. Yüzey desenleri hücrelerin ve hücre salgılarının ve aynı zamanda hücre sitoiskeletinin yönelimli olmalarını sağlamıştır. Yapılan mekanik testler, 21 günlük bir zaman aralığında, keratosit varlığının filmlerin gücünü arttırdığını göstermiş ve biyobozunumun hücre büyümesi ve hücredışı matriks salgılanmasıyla karşılandığını göstermiştir. Ayrıca ışık geçirgenliği bakımından desenli filmlerin

desensiz filmlere göre daha iyi olduğu gözlemlenmiştir. Sonuç olarak, çalışma için tasarlanmış desenlere sahip kollajen filmler başarıyla üretilmiş, bu filmlerin hücreleri ve hücre salgılarını yüzey desenleri içine sınırladığı belirlenmiştir. Desenlerin hücre varlığında yapının ışık geçirgenliği üzerinde olumlu etkisi olduğu saptanmıştır. Elde edilen bilgilerle üretilen taşıyıcıların kornea stroması hücrelerin büyümesi ve bulundukları çevreyi yeniden şekillendirmeleri açısından uygun olduğu ve tüm yapay kornea uygulamalarında başarıyla kullanılabilecekleri sonuçlarına varılmıştır.

Anahtar Kelimeler: Doku Mühendisliği, Kornea, Kollajen, Mikrodesen, Temas yönlendirimi

To My Family

ACKNOWLEDGEMENTS

I wish to express my sincere gratitude to my supervisor Prof. Dr. Vasıf Hasırcı, for his continuous support, guidance and help throughout this study.

I would like to thank Dr. David Hulmes for his contributions to this study both as my co-supervisor and Cornea Engineering project director.

I wish to thank Prof. Odile Damour and Nicolas Builles for supplying human keratocytes and their hospitality during my insightful visit to Dr. Damour's laboratory.

I would like to thank to Dr. Ahmed El-Sheikh for our collaboration in mechanical tests. It was a long and rigorous set of experiments which I am grateful to have been involved in. I am also grateful for his help and hospitality during a part of these experiments which I participated in his laboratory.

I am very grateful to Prof. Atilla Aydınlı for his help in the manufacturing of patterned templates.

I would like to thank my labmates for their help, support and understanding. Pınar Zorlutuna, Pınar Yılgör, Buket Başmanav, Oya Tağıt, Deniz Yücel, Halime Kenar, Nihan Öztürk, Albana Ndreu, Erkin Aydın and Dr. Mathilde Hindie; they have all contributed to this study in one way or another.

I would also want to thank all the undergraduate students, especially Hande Koçak and Pelin Gülay, who have worked with me. Their presence was quite helpful.

I am grateful to Dr. Ayşen Tezcaner for her advices and contributions in the initial phases of my study.

I am grateful to the EU FP6 Project "Cornea Engineering" through which both I and the research was funded.

I would like to acknowledge METU Central Laboratory for analyses done in their facilities.

I am also grateful to TÜBİTAK for their support through BİDEP 2210 Scholarship.

TABLE OF CONTENTS

LIST OF TABLES

LIST OF FIGURES

NOMENCLATURE

Abbreviations

BSA	Bovine Serum Albumin
CLSM	Confocal Laser Scanning Microscope
DMEM	Dulbecco's Modified Eagle's Medium
DAPI	4',6-Diamidino-2-phenylindole
ECM	Extracellular Matrix
EDC	(N-Ethyl-N'-[3-dimethylaminopropyl]carbodiimide)
FITC	Fluorescein Isothiocyanate
IS	Insoluble
LASIK	Laser Assisted *in situ* Keratomileusis
MTS	3-(4,5-dimethylthiazol-2-yl)-5-(3-carboxymethoxyphenyl)-2-(4-sulfophenyl)-2H-tetrazolium
NHS	N-hydroxysuccinimide
OD	Optical Density
PBS	Phosphate Buffered Saline
PLLA	Poly(L-lactic acid)
PLGA	Poly(lactic acid-co-glycolic acid)
PMS	Phenazine Methosulfate
PRK	Laser Photorefractive Keratectomy
RT	Rat Tail
SEM	Scanning Electron Microscope
SMA	Smooth Muscle Actin
UV	Ultraviolet

CHAPTER 1

INTRODUCTION

1.1 Cornea

1.1.1 Structure, Function and Composition of the Cornea

The cornea is the outermost layer of the eye and together with the eyelids and sclera protects the inner part of the eye. Most of the focusing power of eye is due to the cornea. It is an elastic, non-vascularized tissue, about 500-600 micrometers thick, that conforms to the curvature of the eye (Liu et al,1999) and is composed of five distinct layers and three different cell types (Figure 1.1).

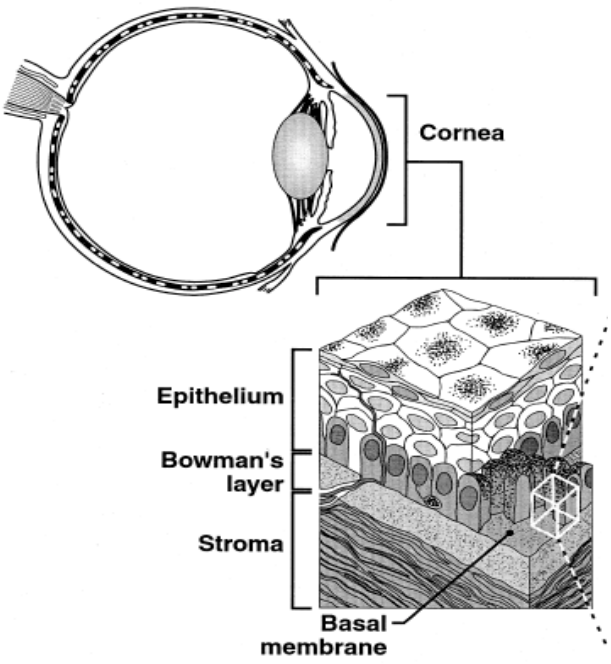

Figure 1.1 Structure of the cornea and its components. Only the upper three layers are shown (Germain et al., 2000).

The anterior part of the cornea contains squamous stratified epithelial cells on a basal membrane. The epithelial part is responsible for protection of the eye from physical agents such as dust and germs. It also provides a smooth surface that facilitates oxygen and nutrient transport to the deeper layers of the cornea. Beneath the basal membrane, there is Bowman's layer which is transparent and composed of collagen fibrils. The corneal stroma is the thickest part of the cornea and is composed of regularly arranged collagen fibrils, which are essential for its transparency. Beneath the stroma, another collageneous membrane called Descemet's membrane exists. This membrane protects mainly against penetration of infectious agents down to the endothelium (Jakus, 1956) and it is secreted by the endothelial cells lying beneath it. The endothelial cells are responsible of the liquid balance within the cornea which is rather critical as overhydration of stroma may lead to corneal opacity. Thus endothelial cells act as a compensating pump that regulates the amount of the liquid within the cornea (Figure 1.2). Liquid balance is also critical because the cornea is avascular and nutrition of the cornea is dependent upon the tears and the aqueous humor (Cursiefen et al, 2003). Avascularity is an important property and is essential for the function of the cornea, since the presence of blood vessels would hamper the transparency of the corneal structure.

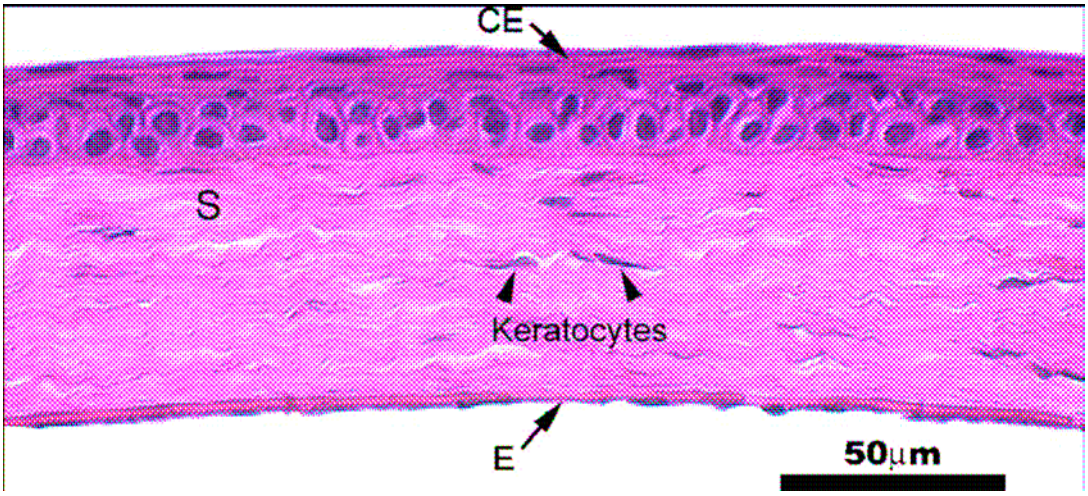

Figure 1.2 Distribution of cells within the cornea (West-Mays et al, 2006). CE: Corneal epithelial cells, S: Stroma, E: Endothelial cells.

1.1.2 Structure and Properties of the Corneal Stroma

The corneal stroma is a 500 micrometer thick tissue that consists of around 200 lamellae arranged orthogonal to each other and perpendicular to the path of light. Keratocytes are interdispersed in this structure and responsible for the turnover of the collagens and proteoglycans present within the stroma. Collagen fibrils, which are composed of collagens type I and V, have uniform fibril diameters and their spacing is quite regular (Figure 1.3). Each lamella is perpendicular to the subsequent one and this orientation is conserved throughout the corneal stroma thickness except in the anterior and the posterior regions (Figure 1.4).

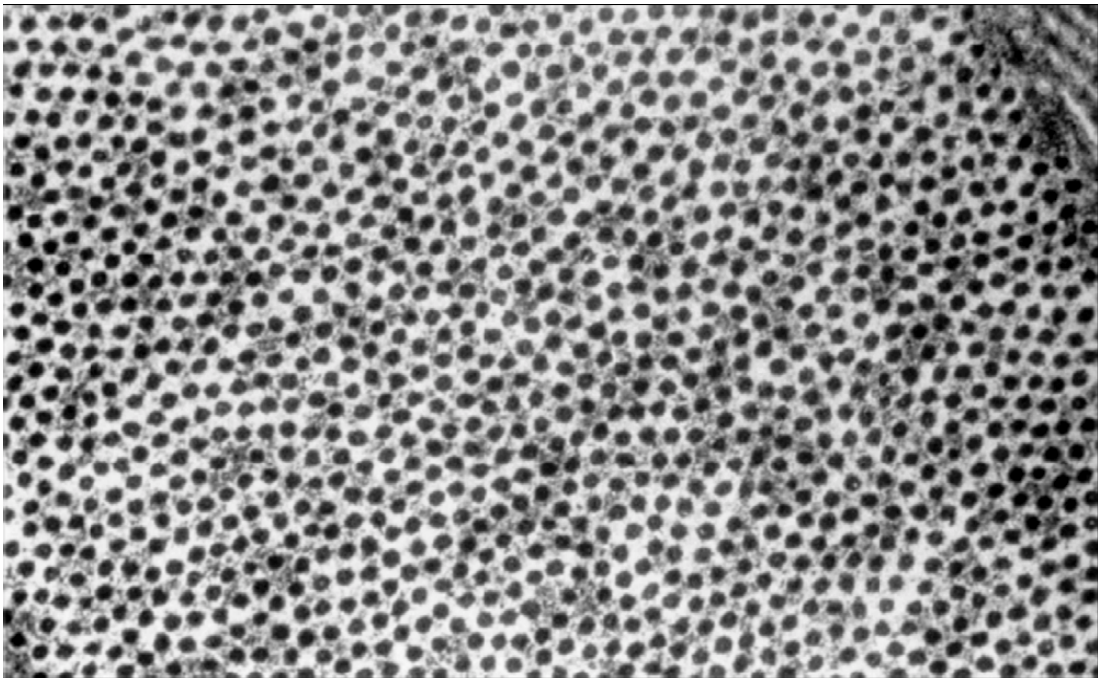

Figure 1.3 Parallel orientation of collagen fibrils, observed in transverse section, in a lamella of corneal stroma (Robert et al, 2001).

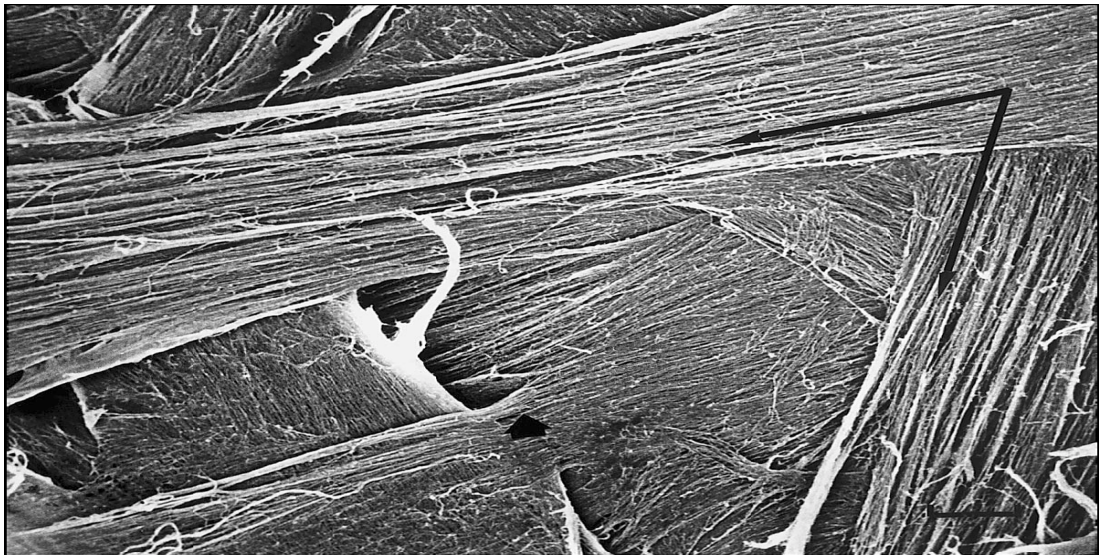

Figure 1.4 Perpendicular orientation of lamellae in corneal stroma (Meek et al, 2001).

The second important constituent of the corneal stroma extracellular matrix (ECM) are the proteoglycans, which include keratocan, lumican and biglycan. These proteoglycans are thought to be involved in the control of spacing of the collagen fibrils. Their absence has been reported as a possible cause of loss of transparency in several occasions, and knock-out mice (lumican deficient) develop corneal haze (Chackravarti et al, 2000). They are generally found perpendicularly aligned with respect to the collagen fiber in each lamellae and are more randomly distributed within the thickness of the corneal stroma. Their presence thus affects the overall structure of the corneal stroma. Also, as do the other proteoglycans, they play a role in the maintenance of stromal hydration (Funderburgh, 2000).

The highly oriented structure of the corneal stroma is an important factor in both corneal transparency and mechanical stability (Meek et al, 1993; Dupps et al, 2006). Corneal transparency is directly related to the regular spacing and distinct diameter of the collagen fibers (Maurice, 1956). Normally, the refractive index of the collagen fibrils is high, thus, a layer of collagen fibrils is expected to scatter light; however this would only hold true if collagen fibrils were distributed randomly within the stroma. However, due to the small diameter and short-range order in the fibrillar organization, this scattering is reduced by the

phenomenon of "destructive interference". This is further confirmed by the diseases that disrupt this intricate organization and cause corneal opaqueness. Furthermore keratocytes contain crystallins such as aldehyde dehydrogenase and transketolase; which are shown to be highly expressed in cornea and these crystallins also contribute to the transparency of the cornea (Jester et al, 1999). This fine ultrastructural control is the essence of the functionality of the cornea. The second important parameter is the hydration level of the collagen fibrils. This is around 78% under normal conditions and *in vitro* examinations have shown that increases in water content also causes a rise in light scattering. This is generally explained by the disruption of the short range order of the corneal collagen fibrils (Clark et al, 2004).

1.1.3 Corneal Keratocytes

Keratocytes are mesenchyme-derived cells that are responsible for the organization and turnover of the corneal stromal ECM; hence they are essential for the transparency of the cornea. There are around 2.5×10^6 keratocytes within the corneal stroma. Corneal keratocytes are themselves quite transparent; which is generally related to the high expression of crystalline proteins such as aldehyde dehydrogenase type III. Under normal conditions, keratocytes are quiescent and have a stellate, flattened shape with long and interconnecting extrusions. In injured cornea, these cells have the ability to change their phenotype (Jester, 2003) into a more fibroblastic one in order to increase the synthesis of the extracellular matrix components that are necessary for the regeneration of the wound area. However, the extent of the injury and the presence of the different signals direct keratocyte behavior such that extensive corneal damage may induce keratocytes to secrete unorganized ECM which may result in corneal haze (Funderburgh et al, 2003).

Upon injury, keratocytes close to the injury site go into apoptosis to prevent further propagation of the injury (Wilson et al, 1998). Remaining cells enter into the cell cycle, gradually losing their dendritic shape and beginning to show more fibroblastic characteristics such as elongated, spindle–like shape, aggressive proliferation and increased ECM secretion. The repair transition also affects the transparency of the keratocytes, since fibroblastic conversion decreases the expression of crystallins. This fibroblastic conversion may lead to either fibroblastic or myofibroblastic phenotypes. Myofibroblasts become bigger

after conversion and they can be distinguished by the presence of smooth muscle actin (SMA) fibers. These cells are responsible for wound contraction and like the fibroblastic phenotype they secrete extensive extracellular matrix components. None of these phenotypes, just like the keratocyte phenotype, is terminal and following regeneration these cells can become keratocytes again. These conversions are generally regulated by the epithelial cells; but cell-ECM interactions have also been shown to be effective in triggering such conversions (Fini et al, 1999).

1.1.4 Corneal Diseases and Dystrophies

Cornea associated problems can be due to physical damage such as etching by strong acids, bases, over-exposure to UV light or genetic diseases and fungal and bacterial infections. Although cornea is quite a resilient tissue with significant regenerative capabilities in some cases, extensive damage cannot be repaired by the usual approaches. Genetically inherited dystrophies can also cause damage in the later stages of a patient's life.

Corneal infections are quite infrequent but can happen due to contaminated contact lenses, and penetration of fungi or bacteria into the cornea can cause severe damage which may lead to loss of corneal transparency and even result in corneal scarring (Chalupa et al, 1987; Huang et al, 2003). These events, generally described as keratitis, can generally be solved by antibiotic or antifungal treatment but there have been cases where permanent damage was incurred too. There are also viral infections of the cornea; such as ocular herpes and shingles which can cause significant damage (Wilson et al, 1997).

There are several genetically inherited corneal dystrophies. These dystrophies generally affect the cornea gradually over time and might not lead to permanent damage. Fuch's dystrophy is one of the most common of several corneal impairments and starts with the detachment of the endothelial lining causing the swelling of the corneal stroma and subsequently its hydration. This eventually leads to severe pain as hydration produces significant pressure within the cornea, and also to blurred vision (Adamis et al, 1993). Although it is a fairly slow-pace dystrophy, this may lead to total dysfunction of the cornea in elderly people. Another dystrophy is keratocunus and can be defined as thinning of the cornea (Kim et al, 1999). It generally starts within the stroma and gradually

affects the curvature of the cornea causing visual impairment. Mild cases can be treated with lenses, however one fourth of the patients generally have extensive distortions that need surgical intervention. Lattice dystrophy is due to synthesis of unorganized fibrils within the stroma which in turn cause accumulation of these proteins and leading to haziness. Another syndrome which is generally related to long-term UV exposure is ptergyism which is the development of a pinkish coloration within the cornea. When small, this growth generally does not obscure visual acuity; however, when larger, deterioration can be severe.

The final major cause of vision loss due to corneal impairment is exposure to chemical agents such as strong acids and bases, high penetration capability of which can rapidly cause severe damage making it impossible for cornea to recover.

1.1.4 Remedies for Cornea Related Health Problems

Some of the corneal dystrophies can be solved with Laser Photorefractive Keratectomy (PRK) a method which has shown great promise but which is not suitable in all cases. When the cornea is irreversibly damaged, the most widely used solution is cornea transplantation. Since the cornea is an avascular tissue, the possibility of rejection is quite low and this makes the cornea a superb tissue for organ transplantation (Claesson et al, 2002). The main problem about cornea transplantation is donor shortage which has become more significant with the widespread use of corneal operations such as Laser Assisted *in situ* Keratomileusis (LASIK) which renders donated corneas unusable. Other problems are disease transmission from the donor tissue and possible function loss during storage.

To overcome these problems several prostheses have been devised over the last 20 years. These systems, generally referred to as keratoprostheses, substitute for corneal functions of transparency and physical protection. Application of keratoprostheses started in the 19th century with the unsuccessful attempts made with glass implants. In the 20th century, several polymers such as polymethylmethacrylate (PMMA), polyvinyl alcohol (PVA), poly(2-hydroxyethyl methacrylate) (PHEMA) have been used to develop keratoprostheses (Chirilla et al, 1998). The most prominent among these is the AlphaCor, previously known as the Chirilla keratoprosthesis (Chirilla et al, 1998). The building block of

AlphaCor is PHEMA and it is composed of two distinct components; the central optic and the skirt. The central optic is composed of a crosslinked PHEMA gel and the skirt is a porous PHEMA sponge. While the central part acts as the main corneal substitute, the skirt allows the integration of the keratoprosthesis with the surrounding tissue due to the permissive nature of the porous structure to cell migration (Hicks et al, 2000). AlphaCor has been developed over the last 15 years and successfully applied in the clinic to several blind patients (Hicks et al, 1998; Eguichi et al, 2004). Another group of keratoprostheses called osteo-odonto keratoprostheses has been in use for the last 30 years (Ricci et al, 1992).

The advantages of keratoprostheses are their availability, ease of storage and production. However, their integration with the body, their susceptibility to infection and their effectiveness always remain in question. Keratoprostheses can be evaluated in the context of first generation biomaterials; their main problem is they are not removable and this can make them a liability when long lifespan expectancy of the population is considered. This is one of the main reasons behind the recent interest in applying tissue engineering to corneal problems.

1.2 Tissue Engineering

1.2.1 Definition of Tissue Engineering

Tissue engineering is an emerging remedy for irreversible tissue damage that causes great suffering all around the world. Its formal definition is: *"Tissue engineering is an interdisciplinary field that applies the principles of engineering and of life science towards the development of biological substitutes that restore, maintain, or improve tissue or organ function"* (Langer et al, 1993).

Normal restorative systems of the human body may not cope with extensive tissue damage and moreover some tissues such as nerve tissue have a limited ability to regenerate. Methods such as implants or organ transplantation (autografts, allografts, xenografts) have been tried in the past. However, all these approaches have their own shortcomings. For example, prostheses have inherent properties that do not match perfectly with the body and can cause problems such as mechanical failure, additional tissue loss, infection or cancer in the long run. For transplantations and grafts the risk of disease transmission,

tissue rejection and side-effects of long term immuno-suppression are always severe possibilities. Moreover, scarcity of donor tissues is another issue. Thus any method that would provide cheap, dependable, durable and transplantable tissue substitutes would be of great service to patients as well as to physicians.

The main idea behind tissue engineering is to develop artificial tissue that can be transplanted and may serve as a substitute or as a facilitator of normal healing mechanisms without causing any adverse effects. There are two main components of a tissue engineered product; cells and the carrier. The design of a proper carrier for the target tissue, as well as obtaining, expanding and manipulating the cells to be used are of utmost importance in tissue engineering (Lavik et al, 2004).

The general approach is to isolate and expand the target cells *in vitro* and then seed these in a manufactured scaffold (or cell carrier) followed by culturing. This can be done either under static culture conditions or using dynamic bioreactor systems, such as perfusion systems, to imitate the natural environment of the cells (Radisic et al, 2004). The culture conditions can be optimized by addition of bioactive molecules that affect cell behavior. After cells proliferate, establish themselves and remodel the scaffold into the target tissue the product can be transplanted (Figure 1.5).

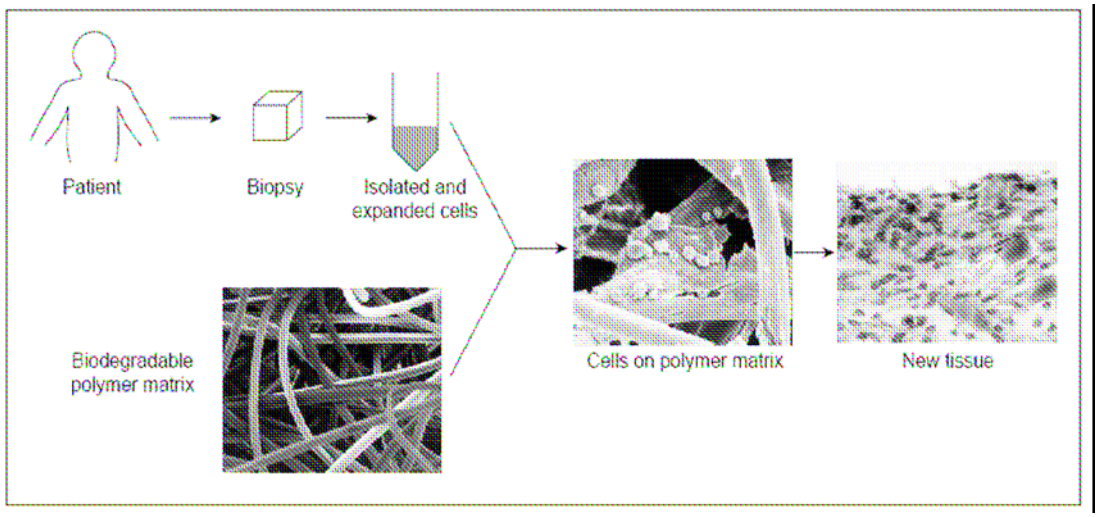

Figure 1.5 A general scheme of tissue engineering methodology (Kim and Mooney, 1998).

Tissue engineering has made significant progress over the last decade and has reached some important goals, such as Food and Drug Administration (FDA) approval of tissue engineered artificial skin and artificial cartilage (Apligraf®: artificial skin, Organogenesis; Cartigel®: Artificial cartilage, Genzyme). Artificial skin has been used in severe burn patients and diabetes related ulcerations for quite some time with success. It is now possible to produce large areas of artificial skin from isolated cells of epidermis and dermis.

1.2.2 Cell Sources for Tissue Engineering

Cell sources can be divided into three: autologous, allogenic and xenogenic. Autologous cells are the patient's own cells, allogenic cells are cells that are expanded from a different person other than the patient, and xenogenic cells are obtained from other species. The most preferred source is autologous cells, because there is a lower risk of inflammation and the immune response is practically nil. Allogenic and xenogenic sources can also be utilized, but with caution. The utilization of embryonic or adult stem cells is an exciting new possibility because these could be induced to differentiate into a range of cell types after manipulation with chemical and biological cues. This is especially helpful in cases where cell isolation is extremely hard.

The decision to use primary or stem cells mainly depends on the proliferation ability of the cell type. Keratinocytes, osteoblasts and chondrocytes can be isolated and expanded from a small biopsy at a reasonably fast rate. This, however is not the case for all cell types. Moreover, expansion can cause dedifferentiation in some cases. Use of embryonic stem cells can solve these problems since they both have a huge self-renewal capacity and a potential for directed differentiation (Bianco et al, 2001). There are certain social and ethical issues concerning the use of embryonic stem cells in tissue engineering, which can partially overcome by the use of adult stem cells. Recently there has been another alternative, called universal cells, which have all their antigenic moieties removed, and thus can be used for all patients (Shieh et al, 2005).

1.2.3 Tissue Engineering Scaffolds

A tissue engineering scaffold can be defined as a 2D or 3D designed structure made of a, preferably biodegradable, material either of synthetic or

natural origin that would provide an hospitable microenvironment for the cells to grow, differentiate and carry out their usual metabolic activity. These materials are generally polymeric, but for hard tissue engineering some inorganic materials such as titanium oxide or calcium phosphates are also being tested. There are certain requirements that should be fulfilled by these materials such as mechanical strength, controllable biodegradability, high porosity and optimum pore size, in order to allow cell infiltration and transfer of nutrients and wastes, as well as sufficient surface area and appropriate chemical and physical surface properties to promote cell attachment, proliferation and migration (Karageorgiou et al, 2005; Chua et al, 2003). In addition, these materials and their degradation products should be biocompatible, i.e. non-toxic, non-immunogenic and non-carcinogenic.

There are several types of materials that satisfy these requirements. Most widely used synthetic and natural polymers for tissue engineering applications are polyesters and the most prominent members of the synthetic group are polyglycolic acid (PGA), polylacticacid (PLA) and their copolymers poly(lactic acid-co-glycolic acid) (PLGA). These materials are FDA approved and their popularity is partially related to this factor. They are being used in the design of scaffolds for tissues like cartilage and bone (Hutmacher et al, 2000; Chen et al, 2006). These polyesters degrade through hydrolytic cleavage of the ester bonds in their structure and their hydrophobicity affects their degradation rate. PGA degrades quite fast (Half-life 20 days; Moran et al, 2003), thus it is not a optimal choice for a large number of applications. On the other hand, PLLA degrades extremely slowly (half-life 300 days, Lu et al, 2000), creating problems due to the long term presence of the degrading polymeric material and its degradation products. Copolymers with different lactic acid:glycolic acid ratios have provided researchers with materials that would degrade in a desired manner depending on the final destination of the tissue engineered product (Kim et al, 1998). Some other polyesters such as polycaprolactone (PCL) (Pena et al, 2006) and polyethyleneterephthalate (PET) (Lu, 2005). are also being used. Natural polyesters for scaffold fabrication are; polyhydroxybutyrate (PHB) and polyhydroxybutryate-co-hydroxyvalerate (PHBV) (Tezcaner, 2003; Kose, 2003). In addition there are polyanhyrides (Gunatillake and Adhikare, 2003), poly(N-isopropyl acrylamide; pNIPAM; Kubata et al, 2006) and polyurethanes (Fromstein and Woodhouse, 2002) which have been shown to be appropriate for tissue engineering applications.

Even though there are several synthetic compounds that almost completely fulfill the requirements for a proper tissue engineering scaffold; the search for better carriers goes on and utilization of natural polymers such as collagen and elastin is desirable since these animal-originated materials naturally embody most of the properties needed (Freyman et al, 2001).

Natural polymers can be human, animal or plant-originated or they may be recombinant. These polymers are mainly polysaccharides and proteins. Structural proteins found in the mammalian body are the most widely used ones. Collagen and elastin have been used in a large number of tissue engineering applications, most notably in skin, bone and cartilage tissue engineering (Lee et al, 2001; Yamauchi et al, 2001; Daemen et al,2003; Ma et al, 2004). In addition to these, other proteins from different sources such as silk have also been tested (Li, 2006). Polysaccharides of the human body include glycosaminoglycan (GAG) molecules such as chondroitin sulfate, dermatan sulfate and hyaluronic acid, and other polysaccharides from other sources such as cellulose, chitosan and alginate are also available (Pek, 2004; Müller, 2006). A third group that has been in use is acellularized ECM models, such as acellularized muscle. These kind of materials have less defined composition but have the advantage of being originally modeled under *in vivo* conditions (Wei, 2005).

Natural polymers, however, pose problems such as inferior mechanical strength, large variation in physical properties, rapid degradation and high cost. Moreover, most of these polymers are hard to process due to their high sensitivity to environmental conditions such as pH and temperature, and animal and plant originated polymers are also induce an immune response.

1.2.4 Scaffold Fabrication Techniques

There are numerous methods to produce two and three dimensional tissue engineering scaffolds depending on the shape, size and level of detail required. For most of the macro-scale tissue engineering scaffolds, porosity is the most crucial factor. There are several ways to produce a porous structure. Basic techniques are porogen-leaching, gas foaming, freeze-drying, fiber bonding, and phase separation (Ma, 2004). There are also "bottom up" techniques which use advances in the field of CAD/CAM (Computer aided design and computer aided manufacturing) to obtain porous structures.

In the porogen leaching technique, a pore former such as sugar or salt is introduced to a hydrophobic polymer solution and the solvent is removed by evaporation. The resulting solid structure is then made porous by dissolving out the porogen (Köse et al, 2003; Liu et al, 2006). Average pore size and porosity of the structure can be adjusted by changing the amount and size of the porogen used (Figure 1.6 a).

In gas-foaming, the structure is filled with a gas such as CO_2 at high pressure and then a sudden drop of pressure which leads to a decrease in the solubility of the gas is used to develop gas bubbles followed by solidification to leave pores behind (Harris et al, 1998; Park, 2002). The amount of the gas dissolved in the solution, rate of pressure decrease and the diffusion properties of the gas in the polymer involved affect the pore size and the porosity.

In freeze-drying, a polymer solution is frozen and then sublimation of the solvent is achieved under very low pressure conditions to produce a porous structure (Sumita, 2006; van Susante, 2001). With this technique structures with more than 90% porosity can be achieved. Pore size and pore distribution are dependent on polymer concentration, type of solvent used and rate of freezing (Figure 1.6 b). With a uniform rate of freezing, highly homogenous structures with a defined pore size can be achieved (Schoof et al, 2001). In fact, freeze-drying is a subgroup of phase-separation techniques in which the main concept is to separate a homogenous system into separate phase and the removal of the one of the phases to attain a porous structure (Mikos and Temenoff, 2000).

Fibrous meshes can be produced by several techniques used in the textile industry along with the new approach electrospinning that leads to nanometer size (diameter) fibers (Zhong et al, 2006). Electrospinning is a process in which a polymer solution is ejected as a jet, with the help of application of an electric potential, from a nozzle towards a grounded receiver surface and settles on this surface as nonwoven fibers (Figure 1.6 c). By changing the operating parameters such as the potential, solvent, polymer type and concentration and the distance between the nozzle and the grounded surface, fibers of desired diameter and nanomats or meshes with high porosity can be produced (Ji, 2006). Their advantages in tissue engineering over other scaffolds are the superior surface area and the relative ease of diffusion due to the high porosity, which allows

better transfer of nutrients. Fiber meshes, however, are generally mechanically weak limiting their utilization. This problem can be overcome by physically bonding the fibers to each other by thermal treatment or after coating the mesh with an another polymer and removing this polymer after bonds are produced (Mikos et al, 1993).

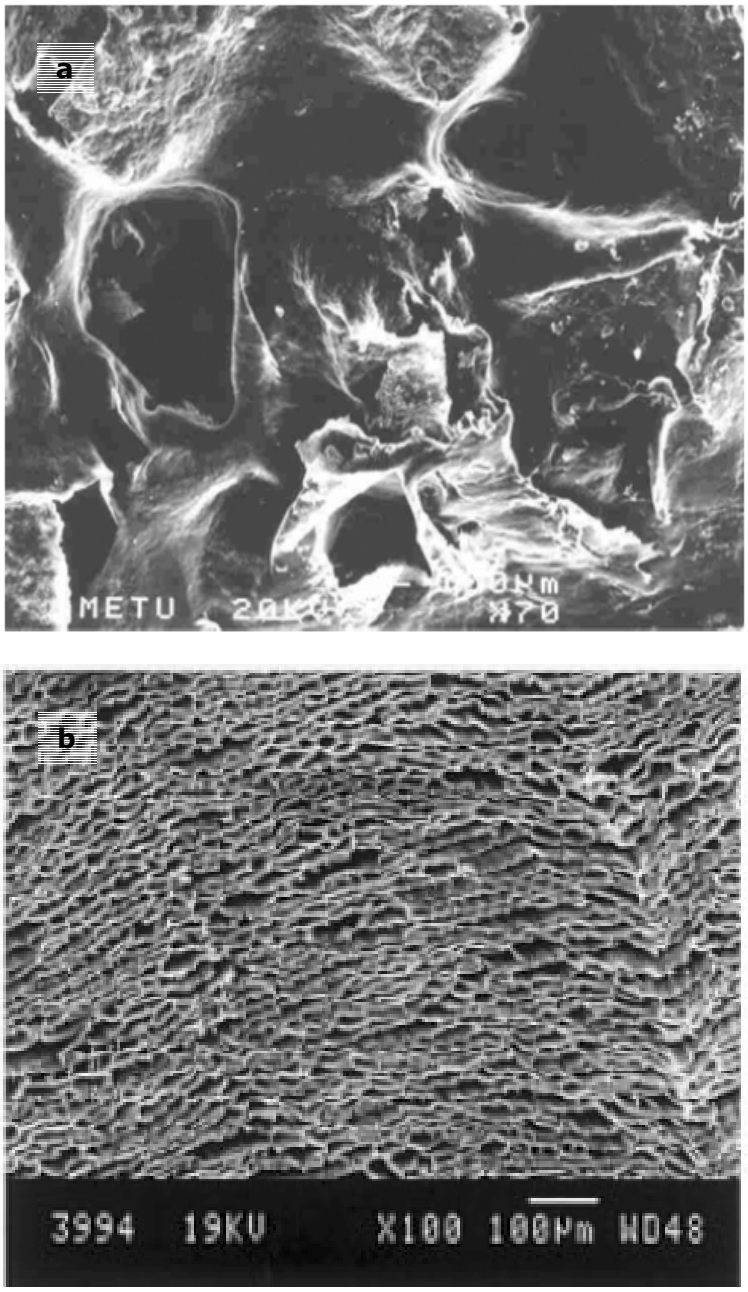

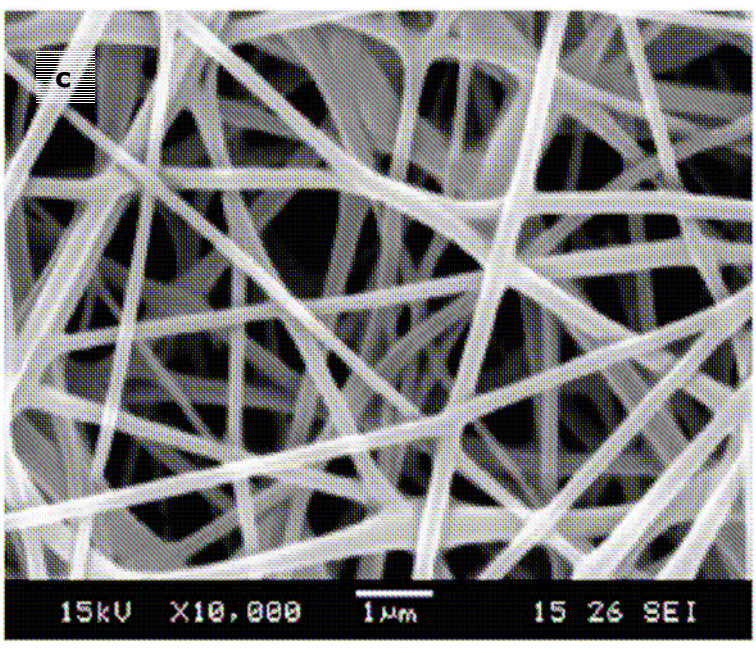

Figure 1.6 Porous scaffolds produced by a) Salt-leaching (Köse et al., 2003), from PHBV; b) Freeze-drying (Maquet et al., 2002), from poly(L-lactide*co*-ε-caprolactone); c) Electrospinning (Zhong, 2006), from collagen-GAG.

General problems with the aforementioned techniques are the limitations of the detail level that can be achieved and difficulty in obtaining a homogenous structure with the desired properties. As mentioned above, techniques that use CAD/CAM technology to realize porous scaffold designs in a layer-by layer fashion have been used to manufacture cell carriers with a pre-determined inner and outer architectures (Tsang and Bhatia, 2004). This can be done by direct methods such as ink-jet printing and rapid prototype printing. Although these are fascinating developments and a precision level of 100 μm has been achieved with such techniques, they are still not widespread and the techniques described earlier are still being used.

1.3 Contact Guidance

1.3.1 Definition of Contact Guidance

Contact guidance is the term that defines the effect of surface properties, such as topography, roughness and presence or absence of bioactive molecules on cell behavior. Contact guidance phenomena have been widely reported in

both *in vivo* and *in vitro* conditions since being first defined by Harrison at the beginning of 20th the century (Harrison, 1912). Cells respond to surface topography and roughness and this response can direct cellular activities such as locomotion, spreading, differentiation and extracellular matrix secretion. Cells can recognize surface patterns down to nanometer scale and this property has been tested with several cell types to achieve their alignment. Reaction of the cells to a physical (3D) surface form depends on the dimensions and the shape of the patterns (Curtis, 1987). If the pattern is that of successive grooves and ridges and if the ridges and grooves are in the low micron range, cells generally settle down and align themselves along the direction of the grooves. Upon decreasing the pitch and the dimensions of the pattern, the same behavior can be established on top of the ridges. More detailed observations have shown that such cellular orientation has a direct effect on cell cytoskeleton, and labeling of focal-adhesion forming proteins such as vinculin also shows alignment of the focal adhesions (Walboomers, 2001). Moreover, such patterns have been found to influence guidance of newly secreted extracellular matrix (Manwaring et al, 2003). The effect of patterning on cell growth is generally not significant and generally correlates with that of unpatterned surfaces (Wan, 2004). But in several cases, patterning has been shown to affect the rate of cell differentiation (Kenar et al, 2006) and to enhance the development of the engineered tissue. Examples are increased matrix deposition and calcification (Matsuzaka, 2003), enhanced myotube formation with aligned myofibroblasts (Lam, 2006), neuron migration (Bellamkonda, 2006) and differentiation of bone marrow stem cells and neural progenitor cells (Recknor, 2006).

1.3.2 Methods for Micro and Nanopatterning

Microfabrication technologies were first developed in the microelectronics industry to manufacture chips and other machine parts but some of these methods have been modified for production of tissue engineering scaffolds.

The most prominent example of such techniques is photolithography, in which the wafer (generally of silicon) to be patterned is coated with a photoresist and exposed to high energy radiation through a mask and a pattern is obtained on the photoresist. Afterwards the gaps in the photoresist allow the surface to be etched either chemically or physically (Figure 1.7; Falconnet et al, 2006). The resultant patterned wafer can then be used as a template from which an inverse

pattern is obtained after coating it with a polymer solution, drying and peeling. A second possibility is the direct patterning of the bioactive molecules by depositing them on the wafer produced and then removing the photoresist (Yap and Zhang, 2006).

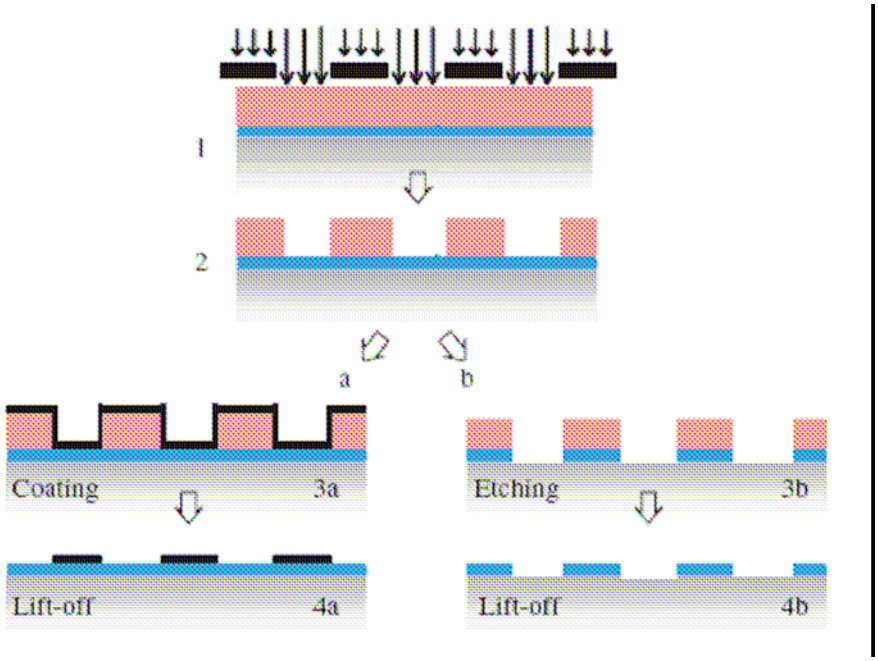

Figure 1.7 Schematic representation of the photolithography technique. The first route is for producing surfaces with patterned bioactive molecules and the second route is for production of patterned templates (Falconnet et al, 2006).

Another widely used method is microcontact printing in which a PDMS replica of the wafer "stamp", is immersed into a solution of a protein or another biologically active molecule and the absorbed proteins are transferred by stamping onto a surface; this way a topographically defined localization of these proteins (such as RGD peptide sequence or cell-adhesion promoting proteins such as laminin and fibronectin) can be achieved (Bhatia, 2000).

Another method to attach proteins on a surface is through using microfluidics in which different solutions are allowed to flow through parallel channels on a template in a controlled fashion leaving behind strips of the proteins contained in the solutions adsorbed on the surface (Khaddemhosseini et al, 2005) This can be achieved either by capillary driven flow, or when this is insufficient, by pressure assisted movement of the bioactive molecule solution.

Microfluidic patterning techniques can also be used for cell micropatterning since the conditions of the process are very mild (Folch et al, 2000).

Achieving nano-scale patterning, techniques such as hot-embossing lithography and nanoimprinting can be used (Lee, 2006). More sophisticated approaches such as electron-beam lithography or nanolithography with atomic force microscope are also available (Hasirci et al, 2006).

All these techniques allow researchers to have a wide range of choices to exploit contact guidance phenomenon on different levels.

1.4 Collagens

1.4.1 Properties of Collagens

Collagens are fibrous proteins. Fibrillar collagens have molecular weights of around 300 kDa. They are a part of extracellular matrix and are secreted by many cell types including connective tissue cells such as fibroblasts. They can be found throughout the body and comprise the most abundant family of proteins in mammals. Currently, 28 different types of collagen have been identified, which differ in the structures of their component alpha chains. These differences cause structural changes affecting self-assembly, fibril formation and network forming capacity (Alberts et al, 2002; Myllyharju and Kivrikko,2001).

1.4.2 Collagen Structure

The collagen triple helix consists of polypeptide chains held together by hydrogen bonding and, in some cases, interchain covalent crosslinks. This results in a superhelical structure which is responsible for the stiffness and stability of collagen molecules. In fibrillar collagens, each alpha chain contains about 1000 amino acids and molecules have lengths of 300 nm. Fibrillar collagens such as the type I collagen, which is the most abundant member of the collagen family, can form large fibrils up to 300 nm in diameter from individual collagen molecules; fibrils can be further strengthened by crosslinking. These fibrils can be as long as several hundred micrometers in normal adult tissues.

The collagen-like motif is rich in glycine, proline and hydroxyproline, all of which are important for the stability of the helical structure of collagen. Every third amino acid residue in the amino acid sequence is glycine whose regular spacing is essential for the tight packing of the superhelical structure. Another distinguishing property of collagen is the presence of hydroxyproline which is specific to collagen.

1.4.3 Function of Collagen

The structure of collagen makes it resistant to tensile forces and in general, collagens are found in the body where there is tensile stress. The arrangement of the collagen fibrils depends on the direction of the tensile stress on the tissues. In skin, collagen fibrils can be found as dispersed bundles since skin elasticity requires resistance to tensile stresses in any direction. On the other hand, for ligaments and tendon whose movement and thus the application of the stress is restricted to one direction, collagen fibrils can be found as regularly arranged bundles in a certain direction, parallel to the stress axis. In bone a similar organization can be observed in which oriented fibrils of collagen also act as carriers for the cells and deposited minerals.

Collagens also provide surfaces for cells to attach and migrate on. This process is quite important in the remodeling of the collagen structure within the tissue because forces exerted on the collagen fibrils reorient and align them in response to the actions of the cells. This is a two-way road in which cellular activities affect the alignment of the collagen fibrils and this causes the alignment of the cells in return. This feature is quite important and is being exploited in tissue engineering applications.

1.4.4. Use of Collagen in Tissue Engineering

Collagens have been utilized by several groups quite efficiently in tissue engineering applications. Perhaps the most notable of these is the use of collagen foams in artificial skin (Freyman et al, 2001). Collagen has been used as an efficient wound dressing material since the first half of the 20th Century; but success in cultivation of human fibroblasts within collagen sponges has shifted the attention toward tissue engineered skin (Jones, 2002). Even though there are established, FDA-approved collagen-based artificial skin products,

studies concerning the optimization of such structures either by changing the production conditions or by addition of complementary materials such as GAGs, the mechanisms behind the remodeling processes (cell population, cell penetration into the matrices, gene expression pattern within the scaffolds etc.) and their *in vivo* performance either in animal models or in clinical trials are still going on (Kuroyanagi et al, 2001;Gingras et al, 2003; Boyce, 2004; Helary et al, 2005;Ng and Hutmacher, 2006).

As one of the most widely used materials in tissue engineering, collagen based matrices have been tried in various applications such as bone engineering, cartilage engineering, muscle tissue engineering, vascular grafts etc. (van Susante, 2001; Yaylaoglu et al, 1999). For cartilage tissue, *in vitro* model studies with collagen foams have shown good cell proliferation and also preservation of chondrocytic phenotype (Pieper et al, 2002; Stark et al, 2006). Collagen foams have also been utilized to repair cartilage defects in *in vitro* model studies and results showed that collagen matrices populated with chondrocytes had a better repair response in comparison to both untreated defects and defects treated with collagen matrix only (Dorotka et al, 2005; Köse et al 2005). Good results were also obtained with chondrocyte seeded collagen gels (Galois et al, 2005).

In bone tissue engineering, collagen scaffolds or collagen containing hybrid scaffolds appear to be very promising. Cell proliferation and differentiation have been observed in collagen gels and collagen films (Wiesmann et al, 2003; Ignatius et al, 2005; Ber et al, 2005). For bone tissue engineering collagen has frequently been incorporated into composite scaffolds. With Collagen/Hydroxyapatite (HAp) 3D scaffolds, three dimensional cellular orientation and new matrix deposition by osteogenic cells was observed (Du et al, 1998. Another collagen-HAp scaffold was also shown to be suitable for osteoinduction and osteoconduction (Rodrigues et al, 2003).

Collagen has been used in a variety of forms such as foams, gels, films, fibers or as composites and also in combination with several other materials such as elastin, chondroitin sulfate and polymethylmethacrylate (PMMA) (Pieper, 1999; Harada, 2000). Not only collagen but also gelatin (denatured collagen) has been successfully used in cartilage tissue engineering applications. Collagen matrices loaded with bioactive agents such as growth factors have been utilized

for applications like cartilage tissue engineering (Lee, 2004). In general, collagen based scaffolds are good for cell adhesion and proliferation, but have low mechanical strength and are rapidly degraded unless stabilized via crosslinking (Angele, 2004; Lee, 2001). Also, there are large discrepancies between the properties of collagens from different sources. Thus, research on the behavior of different cell carriers produced with collagens from different sources, novel scaffold structures, and development of new crosslinking techniques continues (Itoh et al, 2001; Tsai et al 2002, Yunoki et al, 2004; Chen et al, 2005).

1.4.5. Tissue Engineering Approaches for Cornea

There have been several attempts to produce corneal equivalents via tissue engineering. For the epithelial layer, studies have focused on the production of surfaces that are conducive for proliferation of epithelial cells and cues that would lead to total coverage of the surface. To this end, fibrin, epidermal growth factor (EGF) coated polydimethylsiloxane (PDMS) films and crosslinked collagen gels have been used (Rama et al, 2001; Klenkler et al, 2005; Duan and Sheardown; 2006). PDMS films and collagen gels have performed well under *in vitro* conditions and the fibrin substrate has gone through clinical trials with considerable success.

As corneal stroma substitutes, thick dermal collagen type I foams have been produced and these matrices when seeded with human keratocytes showed good cell proliferation and mechanical properties (Orwin, 2000; Orwin, 2003). Collagen hydrogels have also been tried and but even though they had superior transparency, they were mechanically weak (Li, 2004). In another attempt (Germain et al., 1999), corneal keratocytes were seeded within a collagen type I and type III gel; this resulted in quite a transparent structure but contractile activities of the keratocytes contracted the gel. Interwoven PGA meshes seeded with keratocytes were studied under *in vivo* conditions and clarification of the implant was observed in a four month period (Hu, 2005). Although all these trials have had promising results; there is not a definitive artificial cornea design.

In this study; three different collagen based scaffolds (two foams of a constant thickness produced from two different collagen sources and one micropatterned collagen film) were assessed for their suitability as cell carriers for keratocytes to construct an artificial corneal stroma. Two different collagen

foams with a pre-defined thickness (between 500 and 700 μm) were produced. Due to the fact that the natural corneal stroma structure is highly oriented; the substitute corneas should carry physical (3D) patterning to mimic the natural tissue. The effect of micropatterning on cell behavior (cell alignment, ECM secretion) and effects of cell response to physical cues (carrier transparency, mechanical strength) have been tested to determine whether incorporation of micropatterns in an artificial cornea design would be beneficial especially when tested as a stroma. Results have shown that collagen foams made of collagen type I isolated from bovine trachea (insoluble) or rat tail (soluble) were suitable for keratocyte growth; but development of transparency was slow. On the other hand, micropatterning was effective both in achieving transparency and improvement of the mechanical properties of the films. Thus it was concluded that micropatterning should be integrated to the design of a 3-D corneal scaffold to facilitate the remodeling process.

CHAPTER 2

MATERIALS AND METHODS

2.1 Materials

Rat tail type I collagen (purity 99%) was bought from BD Sciences (USA). Insoluble collagen type I (from bovine trachea), EDC (N-Ethyl-N'-[3-dimethylaminopropyl]carbodiimide), N-hydroxysuccinimide (NHS), collagenase type IA (activity: 449 units/mg solid), newborn calf serum, trypsin/EDTA, Amphothericin B, monoclonal anti-human collagen type I antibody, glutaraldehyde, cacodylic acid (sodium salt) and DAPI were purchased from Sigma-Aldrich Corporation (Germany). Fetal calf serum, Dulbecco's Modified Eagle Medium (DMEM; low glucose) were obtained from PAA (Austria). Alexifluor488 conjugated anti-mouse Ig antibody was from Molecular Probes (USA), Anti-human CD34 antibody was bought from Santa Cruz (USA) and b-FGF from Invitrogen (USA). Dulbecco's Modified Eagle Medium (DMEM; high glucose) and Ham's F12 medium were supplied by Gibco (USA). Anti-human keratan sulfate antibody was from Chemicon Inc (USA). Formaldehyde, acetic acid, sodium dihydrogen phosphate and disodium hydrogen phosphate were obtained from Merck (Germany). NucleoCounter reagents were supplied by Chemometec (Denmark) and MTS cell proliferation assay solution was from Promega (USA). Acridine Orange was obtained from BDH Chemicals Ltd. (UK) and Sylgard 184 elastomer solution was from Dow Corning (USA).

2.1.1 Cells

Human corneal keratocytes (primary culture) were provided by Dr. Odile Damour (Cornea Bank of Edouard Herriot Hospital, Lyon, France). D407 Retinal pigment epithelial cells were a kind gift of Dr. R. Hunt (Department of Ophthalmology, University of South Carolina Medical School). For all experiments, keratocytes between passages 4-8 and D407 cells between passages 10-14 were used. Cells were stored in a liquid nitrogen tank.

2.2 Methods

2.2.1 Template Preparation

Silicon templates were manufactured by Prof. Dr. Atilla Aydınlı (Bilkent University Physics Department, Ankara) by photolithography and chemical-etching with the dimensions given below (Table 2.1). Elastomer templates with patterns inverse to the silicon wafers were also produced by the same lab using Sylgard 184 elastomer solution. Solutions were poured on to the silicon templates and after thermal curing (45 min at 100 °C) solidified elastomer was peeled off. Final templates had the inverse pattern dimensions of the template pattern dimensions (Figure 2.1).

Table 2.1 Template dimensions

Groove Depth (μm)	Groove Width (μm)	Ridge Width (μm)	Inclination Angle (degrees)
30	2	10	54.7

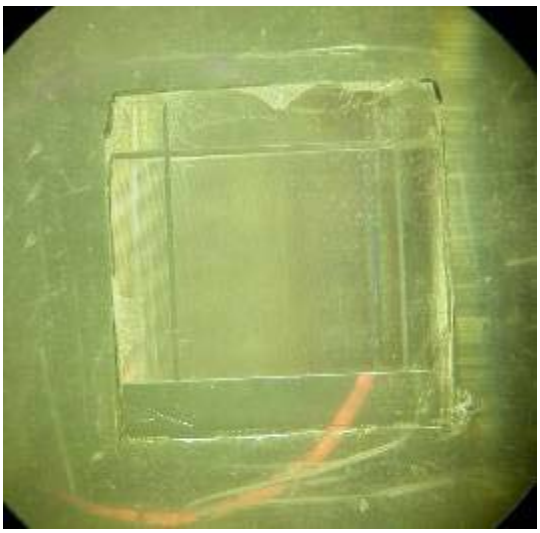

Figure 2.1 Macroscopic appearance of the elastomer template.

2.2.2 Collagen Film Production

2.2.2.1 Micropatterned Collagen Film Production

Micropatterned collagen films were prepared by the solvent casting method. Collagen solutions (15 mg/mL in 0.5 M acetic acid) were prepared by mild agitation at 29 ºC and after total dissolution 200 µL was poured onto the patterned template and air-dried overnight under a hood. Dry films were removed from the template surface using forceps and stored in a desiccator at room temperature until use.

2.2.2.2 Unpatterned Collagen Film Production

For unpatterned collagen films, 200 µL collagen solution was poured onto smooth and flat PDMS surfaces and processed as described above.

2.2.3 Collagen Foam Production

2.2.3.1 Foam Production from Insoluble Collagen

Insoluble collagen (12 mg/mL) was suspended in acetic acid (0.5 M) and then this suspension was homogenized at 900 rpm at 4 °C using a Sartorius Potter S homogenizer for 30 seconds three times with a 30 second pause in between. Final 1 mL aliquots were poured into plastic tissue culture plates and frozen at -20 °C overnight and then lyophilized at -80 °C at 133 $x10^{-6}$ bar vacuum for 8 h (Labconco Freezone Freeze-drier system, USA). Foams were stored in a desiccator at room temperature until use.

2.2.3.2 Production of Foams from Rat Tail Collagen

2.2.3.2.1 Uncrosslinked Foam Production

Rat tail collagen solution (750 µL at 3 mg/mL in 0.02% acetic acid) was poured into plastic tissue culture plates, frozen at -20 °C overnight and then lyophilized at -80 °C at 133 $x10^{-6}$ bar vacuum for 8 h.

2.2.3.2.2 Pre-Crosslinked Foam Production

Rat tail collagen solution (750 µL of 3 mg/mL in 0.02% acetic acid) was poured into plastic tissue culture plates and EDC/NHS solution (100 µL in 50 mM NaH_2PO_4 (pH 5.5) buffer) was added to each plate to reach a final w/w ratio of 1.13/1/1 of EDC/Collagen/NHS. After vigorous mixing, the final solution was incubated for 2 h at room temperature and then lyophilized at -80 °C at 133 $x10^{-6}$ bar vacuum for 8 h.

2.2.4 Scaffold stabilization

Patterned and unpatterned collagen films and insoluble collagen foams were crosslinked by the non-toxic crosslinking method, using EDC/NHS. Scafffolds were immersed into a solution of EDC/NHS (33 mM and 6 mM respectively) in a 50 mM NaH_2PO_4 buffer (pH 5.5) for 2 h at room temperature. Then the pH of the system was neutralized by incubating the scaffolds in 0.1 M

Na_2HPO_4 (pH 9.1) buffer for 1 h followed by washing steps in 2M and 1M NaCl solutions. Lastly scaffolds were rinsed with distilled water several times and air dried.

2.2.5 Scaffold Characterization

2.2.5.1 Film and Foam Thickness Measurement

Film and foam thicknesses were measured using a standard micrometer (Erste Qualitat, Germany) to a sensitivity of 0.1 μm before and after crosslinking. Each sample was measured at least three times and for both crosslinked and uncrosslinked specimens 6 samples were used.

2.2.5.2 Measurement of Surface Porosity of Foams

Porosity of the foams and the presence of a skin layer was assessed from 4 micrographs taken by a Nikon SMZ 1900 Stereomicroscope (Japan) of both the upper and lower surfaces of the foams and porosity was determined by analyzing these images with the NIH Scion image program.

2.2.5.3 Bulk Porosity of foams

In order to determine the porosity of the foams, the volume occupied by the collagen in uncrosslinked insoluble collagen foams and crosslinked insoluble and rat tail foams (6 of each) was determined using a helium pycnometer (Ultrapycnometer 1000, Quantachrome Corporation, USA). Then porosity was calculated as the ratio of the volume of the collagen determined to the volume of the foam calculated from its dimensions.

2.2.5.4 Pore Size Distribution

Pore size distribution of the both crosslinked and uncrosslinked foams were determined using a mercury porosimeter (Quantachrome Corporation, Poremaster 60, USA) under low pressure conditions.

2.2.5.5 Degradation *in situ*

In order to study the degradation profile, scaffolds were incubated under normal culture conditions (in sterile 24 well plates at 37 °C and under 5% CO_2) in sterile 10 mM PBS (pH 7.4). The extent of degradation was examined at time points 1, 2 and 4 weeks with SEM, stereomicroscopy, gravimetry and by medium pH measurements.

2.2.5.5 Stability of Scaffolds: Collagenase Assay

To study the resistance of patterned collagen films to enzymatic degradation, pre-weighed films were incubated in collagenase A solution (0.1 mg/mL in sterile PBS pH 7.4) for periods of 1, 2 and 3 h. Films were then rinsed several times with distilled water and weighed after lyophilization to determine weight loss.

2.2.6 SEM examination

All samples were examined by SEM. Unprocessed scaffolds were stuck after excessive rinsing with cacodylate buffer (pH 7.4), lyophilized, gold-coated under vacuum with a sputter coating device (Hummle VII, Anatech, USA) and observed with scanning electron microscope (JSM 6400, JEOL, Japan).

2.2.7 *In vitro* Studies

2.2.7.1 Cell Culture

All cells were stored frozen in a liquid nitrogen tank in their respective medium with addition of 15% DMSO until use. Following thawing, cells were used after reaching confluency and passaged one more time. All cell culture experiments were conducted under standard culture conditions. Cells were incubated in a CO_2 incubator at 37 °C and 5% CO_2.

2.2.7.1.1 Keratocyte Culture

Human keratocytes were received in a tissue culture flask in dry ice (passage 2 and passage 4) and propagated until passage 8. In all experiments keratocytes between passage 4-8 were used. The composition of the keratocyte medium for 500 ml was as follows: 225 mL of DMEM high glucose, 225 ml of Ham F12 medium, 50 mL of new born calf serum, 10 ng/mL human recombinant b-FGF, amphotericin (1 µg/ml), streptomycin (100 µg/ml) and penicillin (100 UI/mL).

2.2.7.1.2 D407 Culture

D407 cells between passages 10-14 were used in the experiments. The composition of 500 mL medium was as follows: 475 mL of DMEM high glucose, 25 mL of fetal calf serum, amphotericin (1 µg/ml), streptomycin (100 µg/ml) and penicillin (100 UI/mL).

2.2.7.2 Cell Seeding onto Scaffolds

Cells were detached from the flask surface by treatment with 0.25% trypsin for 5 min at 37 °C. After detachment, trypsin was deactivated with serum and cells were collected by centrifugation. Cells were then counted with a Nucleocounter (Appendix A). After determination of the cell number, 50 µL of keratocyte containing medium was seeded onto each film and foam. For the determination of growth profile, transparency, keratan sulfate content and for DAPI and CD34 staining, $1x10^4$ keratocytes per film were used. For mechanical tests, f-actin and collagen type 1 staining, $5x10^4$ cells were used. For foams $5x10^4$ cells were used. After seeding, the scaffolds were incubated for cell attachment in a CO_2 incubator for 1 h, then at the end of 1 h the volume of the medium was completed to 500 µL under sterile conditions.

2.2.7.3 Cell Proliferation on Scaffolds

To examine cell proliferation on and within the scaffolds, the MTS cell proliferation assay was carried out for each scaffold in triplicate for days 1, 4, 7 and 10. For each time point, the medium was discarded and the well was washed with sterile PBS to remove any remaining medium. Then 10% MTS

solution (500 µL) was added and scaffolds were incubated at 37 °C and 5% CO_2 for 2 h. After 2 h, 100 µL of the solution was transferred to a 96-well plate and absorbance was determined at 490 nm using an Elisa plate reader (Molecular Devices, USA). To correlate the absorbance with the cell number, a calibration curve of known cell numbers was constructed (see Appendix A).

2.2.8 Microscopical Studies

2.2.8.1 Acridine Orange Staining

Keratocyte seeded collagen films were fixed after days 1, 7, 14 and 21 with 2.5% glutaraldehyde solution for 2 h. Afterwards, films were rinsed with PBS and 10% Acridine Orange was applied for 15 min while protecting specimens from light exposure. The specimens were rinsed with PBS and observed using an Olympus IX-70 (Japan) fluorescence microscope with WB filter (450-480 nm). For rat tail collagen foams the same procedure was carried out after 14 days of incubation.

2.2.8.2 DAPI Staining

Keratocyte seeded patterned and unpatterned films and D407 seeded patterned films were stained with the nuclear stain DAPI. After fixation in 4% formaldehyde solution for 15 min, specimens were rinsed with PBS and then DAPI solution (diluted 1:1000 in PBS solution) was applied onto the scaffolds which were incubated at 37 °C in the dark for 45 min. Afterwards, specimens were rinsed with PBS and examined using an Olympus IX-70 fluorescence microscope with WU filter (330-385 nm).

2.2.8.3 SEM Examination

Patterned collagen films seeded with keratocytes after days 7, 10, 14 were fixed with 2.5% glutaraldehyde in cacodylate buffer (pH 7.4) for 2 h and then washed with cacodylate buffer and with distilled water several times and freeze-dried. Afterwards samples were gold coated by sputtering and observed with a scanning electron microscope. The same approach was applied to D407 cells on films and to insoluble collagen foams seeded with keratocytes after day 7.

2.2.8.4 FITC-Labelled Phalloidin Staining

To observe the orientation of cytoskeletal actin filaments, in cells on patterned collagen films, FITC labeled phalloidin staining was performed. This was applied to keratocyte seeded patterned collagen films after 7 days of incubation. Samples were fixed with 4% formaldehyde for 15 min and then washed with PBS (pH 7.4). Cell membranes were permeabilized with a 1% Triton-X100 solution for 5 min. After washing, samples were incubated at 37 °C for 1 h in 1% PBS-BSA solution. After washing, FITC labeled phalloidin (1:100 dilution in 0.1% PBS-BSA) was added and samples were incubated for another 1 h. Samples were transferred to a microscope slide and covered with 50% PBS-glycerol and observed using an Olympus IX-70 (Japan) fluorescence microscope with WB filter (450-480 nm).

2.2.8.5 Immunostaining

2.2.8.5.1 Collagen Type I Staining

In order to study extracellular matrix (ECM) secretion by keratocytes and D407 cells, indirect immunostaining with anti-collagen type I antibody was performed. Films seeded with keratocytes and D407 cells were fixed with 2.5% formaldehyde for 15 min on days 1 and 7. After washing with PBS (pH 7.4), cell membranes were permeabilized with 1% Triton-X100 solution for 5 min. After washing, samples were incubated at 37 °C for 1 h in 1% PBS-BSA solution. Anti-human collagen type I antibody produced in mice (1:200 dilution in 0.1% PBS-BSA solution) was then added onto the specimens followed by incubation for 1 h at 37 °C. Samples were washed with 0.1% PBS-BSA solution and Alexifluor488-labelled Anti-mouse antibody produced in goat (1:100 dilution in 0.1% BSA-PBS) was added and incubated at 37 °C for another hour and then washed with 0.1% PBS-BSA solution. Samples were observed using an Olympus IX-70 (Japan) fluorescence microscope with WB filter (450-480 nm).

2.2.8.5.2 Keratan Sulfate Staining

In order to determine the presence of the keratocyte-specific proteoglycan, keratan sulfate, films seeded with keratocytes were stained for keratan sulfate on days 1 and 7 with indirect immunostaining. Samples were

fixed with 2.5% formaldehyde for 15 min. After washing with PBS (pH 7.4) cell membranes were permeabilized with 1% Triton-X100 for 5 min. Samples were washed with PBS and incubated at 37 °C for 1 h in 1% PBS-BSA solution. After washing, anti-human keratan sulfate antibody produced in mice (1:100 dilution in 0.1% BSA-PBS) was added onto the specimens and samples were incubated for 1 h at 37 °C. Then samples were washed, Alexifluor488-labelled anti-mouse antibody produced in goat (1:100 dilution in 0.1% BSA-PBS) was added followed by incubation at 37 °C for another hour. Washed samples were observed using an Olympus IX-70 (Japan) fluorescence microscope with WB filter (450-480 nm).

2.2.8.6 Confocal Laser Scanning Microscopy (CLSM)

Confocal microscopy (Zeiss LSM 9100, Germany) was used to assess the distribution of cells within the foams and also to visualise the distribution of newly secreted collagen in 3D. Specimens were stained with 10% Acridine Orange and indirect immunostaining for collagen type I was performed as described above. An argon laser was used to excite the dyes and examine the specimens.

2.2.9. Mechanical Strength of Patterned Collagen Films

Patterned collagen films, a) unseeded and incubated under culture conditions, b) seeded with human corneal keratocytes, c) seeded with D407 epithelial cells, were tested using an Instron 3366 tensile tester (Instron Corp., USA) with a strain rate of 0.2 mm/min up until failure. Six specimens for days 0, 7, 14 and 21 for each group were tested. Test sample dimensions were 1 cm x 1 cm x 42 μm and tests were carried out with a special test rig designed and used by Prof. A. El-Sheikh (University of Dundee, UK).

2.2.10. Transparency Measurement

Transparency of the scaffolds was measured using a Shimadzu 2100-S UV-Vis spectrophotometer by scanning in the range 250 nm to 700 nm after fixing the scaffolds against quartz spectrophotometer cuvettes. Transparency of patterned and unpatterned, keratocyte seeded and unseeded films were tested on days 1, 4, 7 and 10. Keratocyte seeded and unseeded rat tail and insoluble collagen foams were tested on days 0 and 7.

2.3 Statistical Analysis

Statistical analysis was carried out by the Student's t-test; $p \leq 0.05$ was considered significant.

CHAPTER 3

RESULTS AND DISCUSSION

3.1 Scaffold Characterization

Before starting the *in vitro* experiments; the physical characteristics of the scaffolds that affect cellular behavior, such as preservation of the patterns after crosslinking, porosity and pore size distribution of the foams and thickness of the carriers, were determined.

3.1.1 Film Characterization

Film thickness was found to be 42.0±0.3 μm. Crosslinking did not have any effect on film thickness. Microscopic observation of the surface showed that fidelity of the pattern was quite high and crosslinking did not disturb the surface pattern (Figure 3.1.a). Crosslinked films were rougher (Figure 3.1.b). This roughness is known to be facilitative for cell attachment, mainly due to the better adsorption of adhesion promoting proteins in the serum to the rougher surfaces (Degasne et al, 1999). This positive effect has been observed with different materials (Lampin et al, 1997; Deligianni et al, 2001), though this benefit can be shrouded by the fact that collagen itself is an adhesion promoting protein.

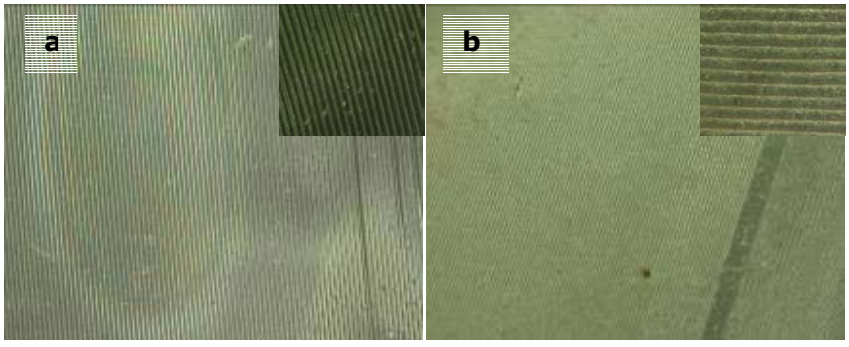

Figure 3.1 Stereomicrographs of patterned collagen films. a) Uncrosslinked, b) Crosslinked. (Magnification 6x), Insets (Magnification 33.75x)

Surface topography of the crosslinked, patterned collagen films was further investigated by SEM (Figure 3.2a). Surface roughness is quite apparent at higher magnifications; oriented striations were observed on the face of the ridges (Figure 3.2b). These striations were too big to be individual collagen fibrils; so they most probably were aggregates of collagen fibrils upon crosslinking.

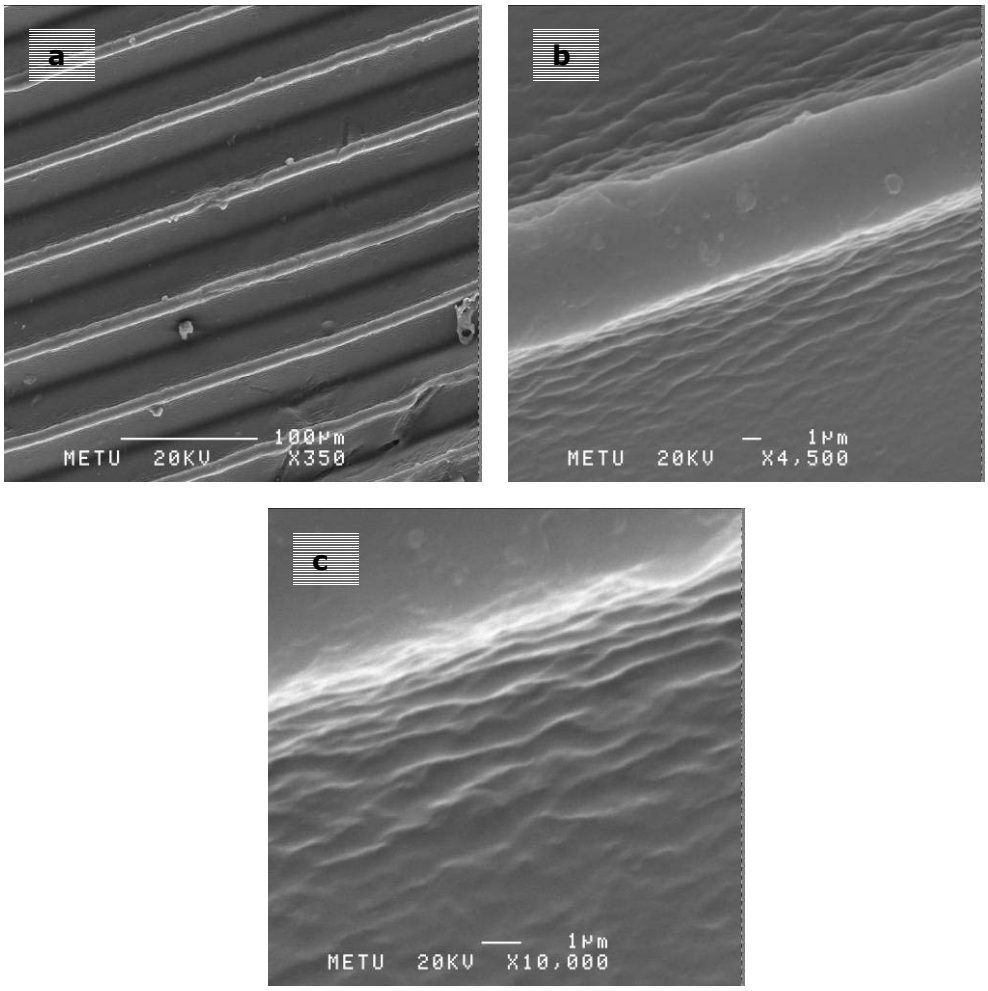

Figure 3.2 SEM micrographs of crosslinked, patterned collagen film. **a)** Overall structure, **b)** Top of a ridge, **c)** Oriented striation at the apex of a ridge.

3.1.2 Foam Characterization

3.1.2.1 Crosslinking

Crosslinking of rat tail (RT) collagen foams with conventional methods (immersion of the scaffold into the crosslinking medium) leads to extreme shrinkage (Table 3.1) and loss of porous structure (Figure 3.3). However, conventional crosslinking did not result in a dramatic change in the thickness of the insoluble collagen foams. Initial and final thicknesses are given in Table 3.1. Other researchers have also observed varying degrees of shrinkage when collagens from different sources were used (Angele et al, 2004).

In order to prevent shrinkage and to have a better control on the final thickness of the foam, the RT collagen solution was crosslinked with EDC/NHS before the resultant foams were made and foams preserved 74.6% of their original thickness (Table 3.1, Figure 3.4). Thickness has not been taken into consideration in the reported designs in the literature, but it is important for the ease of remodeling *in vivo* and it is also crucial during implantation.

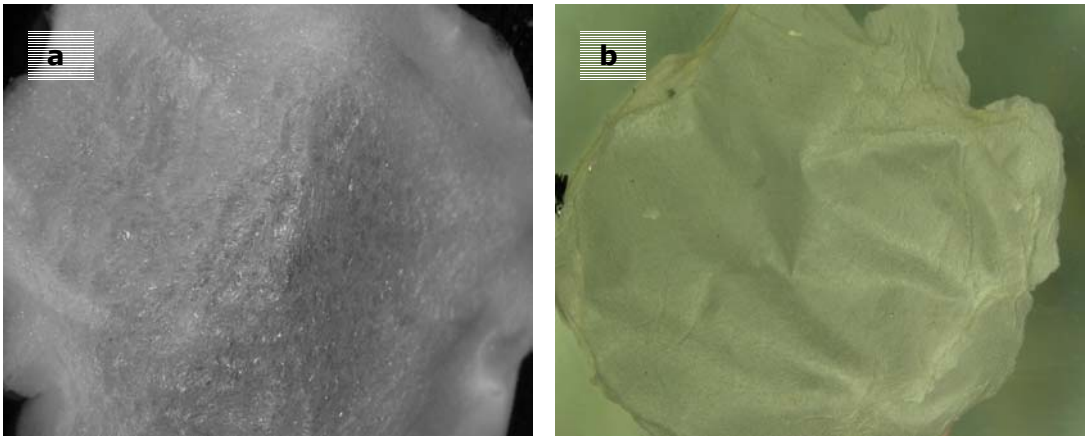

Figure 3.3 Effect of conventional crosslinking on rat tail collagen foams. **a)** Uncrosslinked, **b)** Crosslinked foam (Magnification x 6).

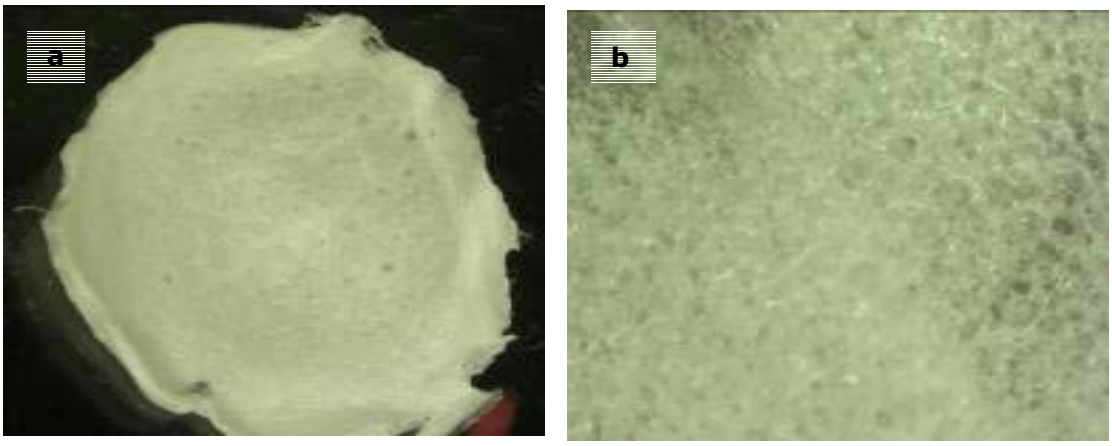

Figure 3.4 Structure of pre-crosslinked collagen foam. **a)** Macroscopic view (Magnification x 6) **b)** Surface characteristics (Magnification x 33.75).

Table 3.1 Foam thickness before and after crosslinking (μm).

Foam type/Treatment	Rat Tail	Insoluble
Uncrosslinked	721±17.6	1150.3±39.6
Crosslinked	72.3±4.1	811.3±25.2
Pre-crosslinked	531.6±23.7	-

3.1.2.2 Surface Porosity

Surface porosity of the collagen foams made from rat tail and the insoluble collagen are presented in Table 3.2. It is a fact that the lyophilization procedure causes the formation of a layer of lower porosity, "skin layer", both at the top and the bottom of the foams. This may adversely affect the cell and nutrient penetration especially when seeding is done using the upper surface. To quantify this effect, upper and lower surface layers of the collagen foams were compared in terms of their porosity using stereomicrographs and an image processing program. The skin layer was present in insoluble collagen foams (but the porosity of the upper surface was high enough for in vitro studies, see Section 3.3). The top skin layer of rat tail collagen foams was more porous than that of the insoluble foams. Slightly higher porosity of the upper part of the rat

tail foams might be due to the crosslinking protocol which might have been more effective in the lower part where exposure to air is less thus decreasing the porosity.

Table 3.2 Surface porosity of foams.

Surface	**Foam type/Porosity (%)**	
	Rat Tail	**Insoluble**
Upper	64.3±8.4	52.1±6.2
Lower	61.8±3.8	64.5±2.7

3.1.2.3 Porosity of the foams

The presence of a skin layer may interfere with the determination of the porosity of a foamy structure via processing of visual information. In order to determine if there is any difference between the surface porosities determined by Scion image and the bulk porosity of the system, the volume occupied by the collagen in the foams were determined. Bulk porosities of the foams are given in Table 3.3.

Table 3.3 Bulk porosity of the foams.

Foam Type	**Porosity (%)**
Crosslinked Rat tail	95.8
Uncrosslinked Insoluble	97.1
Crosslinked Insoluble	93.6

An ideal porous tissue engineering scaffold should have a porosity of at least 90% (Freyman et al, 2001). Both crosslinked foams were over this limiting number and their bulk porosity was higher than their surface porosity, which indicates the presence of skin layer. Crosslinking mildly affected the bulk

porosity but this decrease was not significant enough to compromise the suitability of the foams.

3.1.2.4 Pore Size Distribution

There exists a porosity range in which cell penetration and mass transfer is optimum for porous scaffolds. This fact is related to two parameters; first, pore size affects the cell's migration capability since cells cannot move through pores smaller than their size. On the other hand, for cells to attach firmly and spread themselves, there exists a minimum ligand density necessary for cells to recognize. Thus, with larger pore sizes cells cannot find enough surface to adhere properly (O'Brien et al, 2005). Although there is a significant variation in the optimal pore size between cell types, an optimum range for dermal fibroblasts, which can be used as a general reference for fibroblastic cells, has been previously defined (Yannas et al, 1989). Pore size has been demonstrated to be important for both nutrient and waste transportation and also for cellular behaviour. For example, hepatocytes seeded on collagen foams with a average pore size less than the hepatocyte size (10 μm) were not permissive for cell spreading, penetration and network formation (Ranucci et al,2000). The pore size distribution is also an important factor in determining the homogeneous behavior of the scaffold. To determine the pore size distribution and the effect of crosslinking on pore size distribution, six foams of each type were examined using a mercury porosimeter. Rat tail foams, when uncrosslinked, showed a wide pore size distribution, with an average of 63.8 μm. Crosslinking seems to decrease the breadth of the pore size distribution curve, but, median pore size, 16.6 μm, is less than the optimum range (Figure 3.5a). But the presence of bigger pores might be enough for cellular movement, so the average pore size of 35.6 μm is within the desired values. For insoluble collagen foams, pore size distribution is more uniform and within the expected range (Figure 3.5b). Also crosslinking did not effect the pore size distribution, apart from decreasing the average pore size from 73.5 μm to 67.7 μm and also decreasing the standard deviation. Average pore sizes for both type of foams are given in Table 3.3.

a)

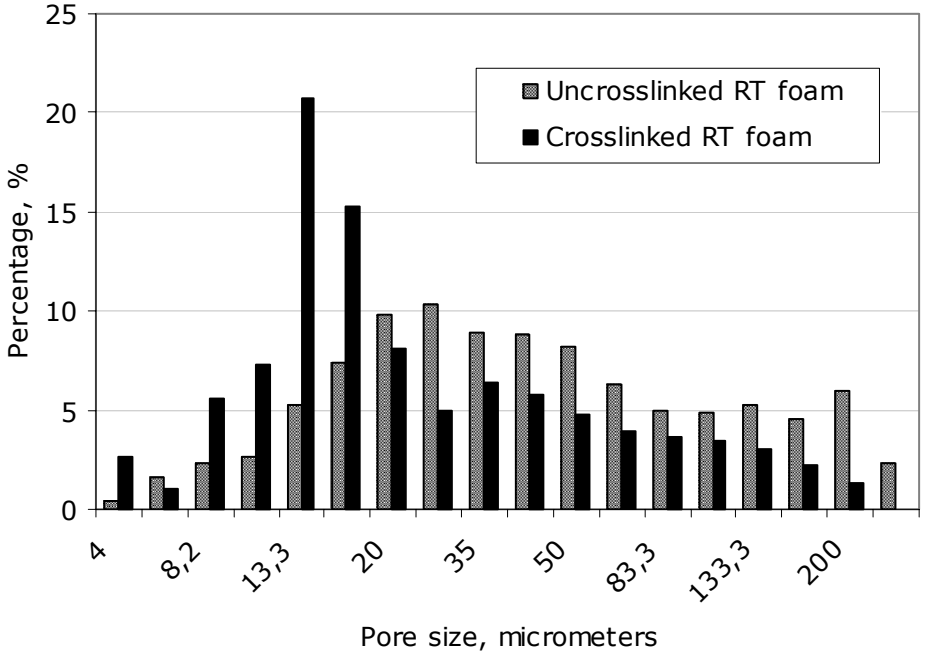

b)

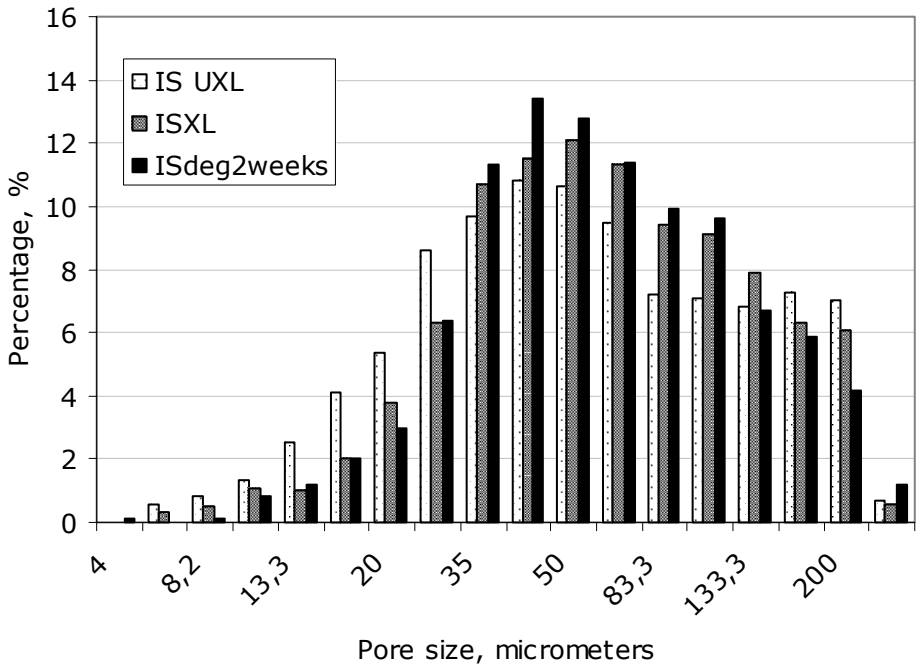

Figure 3.5 Pore size distribution of **a)** Crosslinked and uncrosslinked rat tail collagen foams, **b)** Crosslinked, uncrosslinked and crosslinked-degraded for two weeks *in situ* insoluble collagen foams.

Table 3.4 Average pore size of rat tail and insoluble collagen foams.

Treatment	Average Pore size (μm)	
	Rat tail collagen foam	Insoluble collagen foam
Uncrosslinked	63.8	73.5
Crosslinked	35.6	67.7
Degradation (2 weeks)	-	74.0

3.2 Degradation Profiles of the Scaffolds

For integration of a tissue engineered product with the host, rate of degradation and the effect of degradation on carrier properties are of utmost importance. The scaffold should degrade neither too slow nor too fast, since fast degradation compromises structural stability and slow degradation prevents remodeling, thus decreasing the effectiveness of the scaffold (Pek et al, 2004). Scaffold degradation studies were carried out for a month at 37 °C in PBS (pH 7.4, 10 mM). During this period, the films lost up to 50% of their initial weight. Among the foams there seems to be no significant difference. Both behave in a bi-phasic manner with a total weight loss of ca. 70% in 4 weeks (Figures 3.6). There was a small but steady decrease in pH of the medium, all solutions ending up slightly acidic in 4 weeks due to the formation of acidic groups as a result of degradation (Figures 3.7).

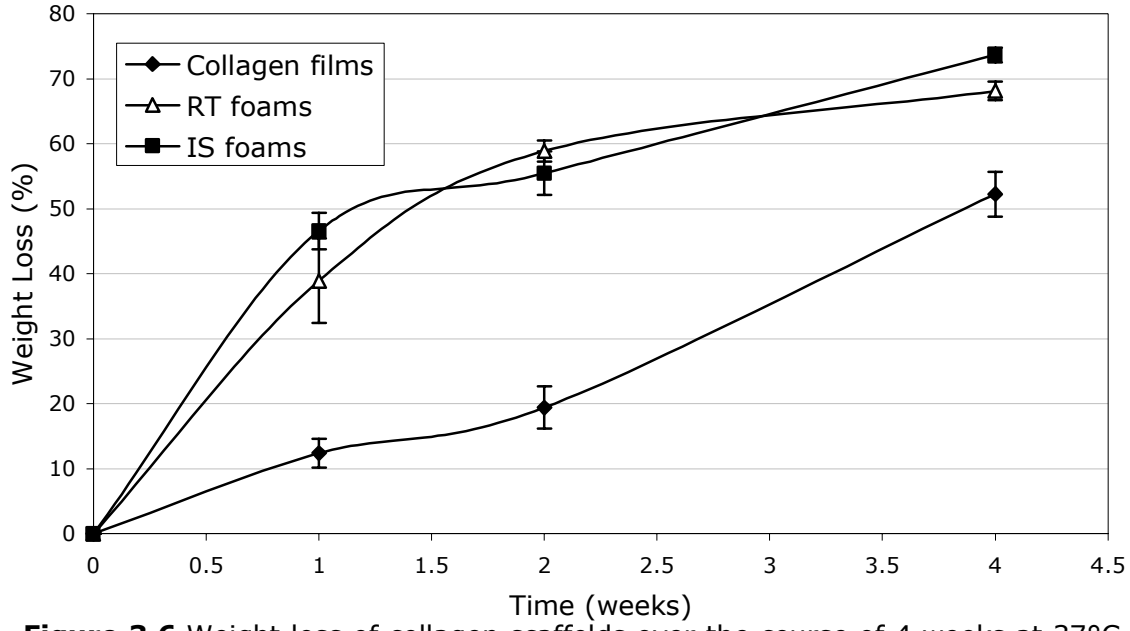

Figure 3.6 Weight loss of collagen scaffolds over the course of 4 weeks at 37°C in PBS (pH 7.4, 10 mM).

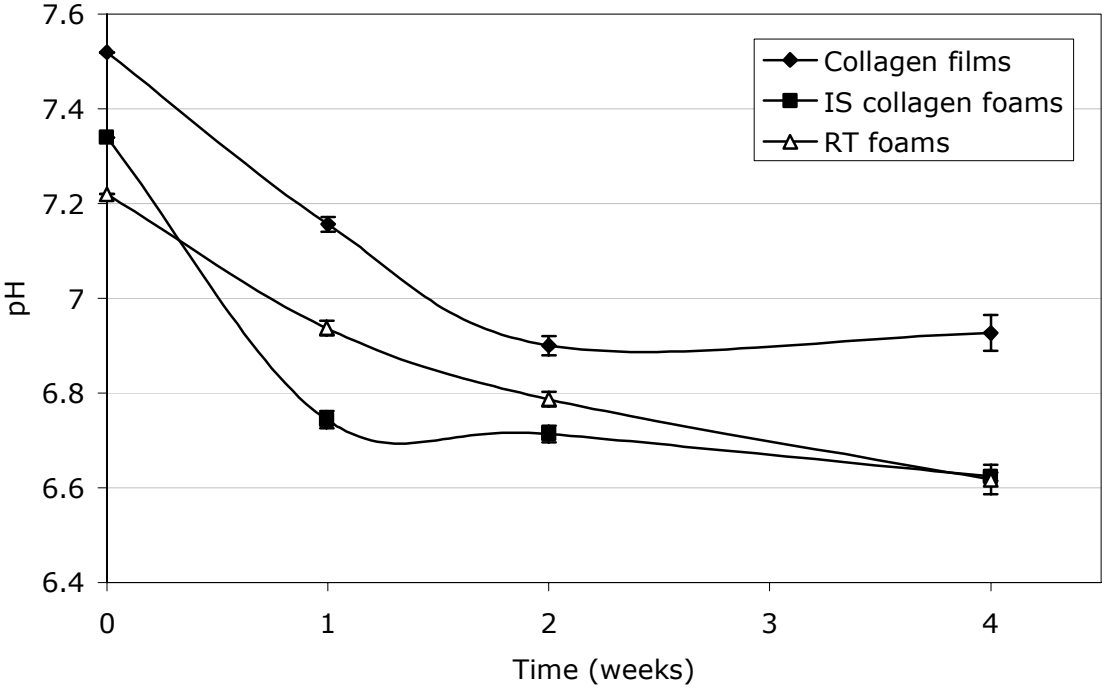

Figure 3.7 pH change of the degradation medium over the course of a 4-week incubation at 37 °C in PBS (pH 7.4, 10 mM).

Stereomicroscopic observations showed little deformation of the patterns on the films over a one month period (Figure 3.8 a,b). However, SEM examination showed extensive pattern deterioration and deposition of material in a one month period (Figure 3.8c,d).

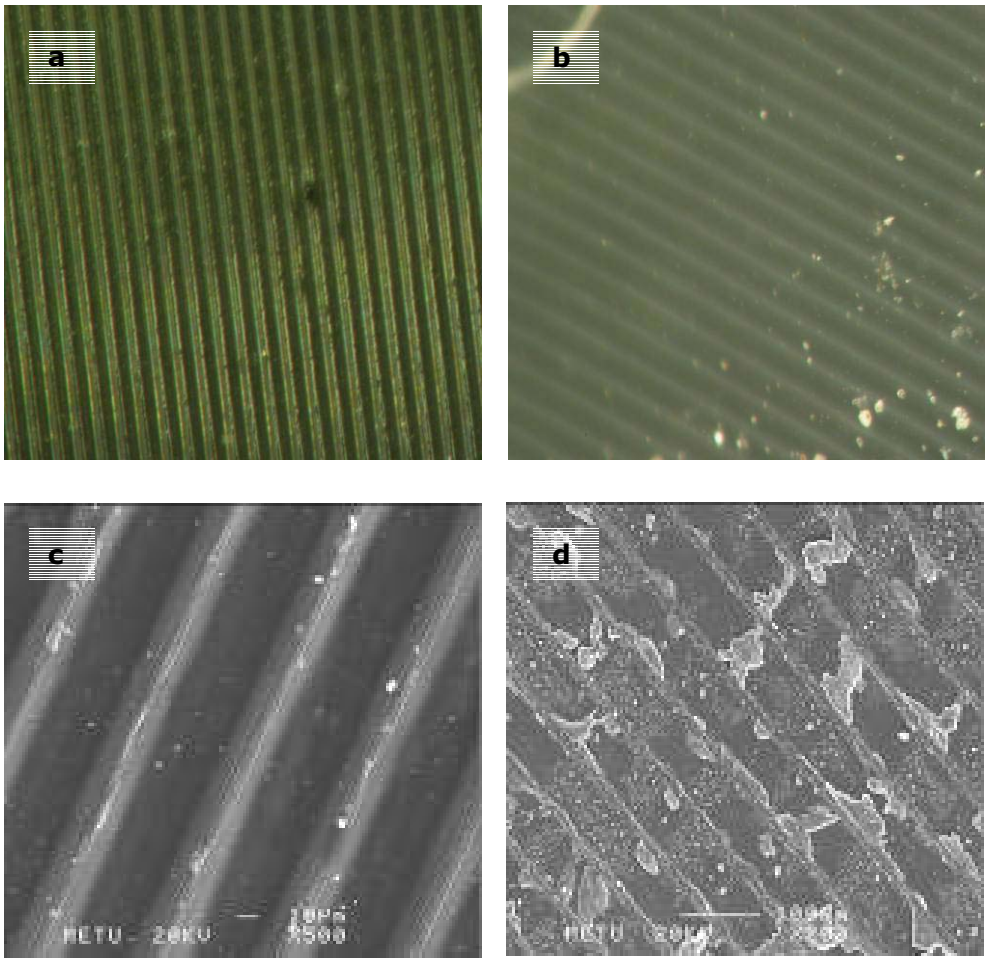

Figure 3.8 Micrographs of collagen films before and after degradation. **a-b)** Stereomicrographs: (a) untreated, (b) after 4 weeks of incubation, (Mag x33.75), SEM micrographs: (c) untreated, (d) after 4 weeks of incubation.

For rat tail foams; SEM examinations demonstrated that degradation increases the porosity and the number of pores and decreases the surface regularity (Figure 3.9a-e). With the insoluble collagen foams degradation was not quite discernible (Figure 3.10a-c); however, cross sectional views of these foams showed an increased deterioration in the inner parts of the foam, as revealed by the decrease in the thickness of the fibers (Figure 3.10d, e). Also

mercury porosimetry measurement after 2 weeks of degradation showed a small increase in the average pore size, from 67.7 μm to 74 μm (Figure 3.5b).

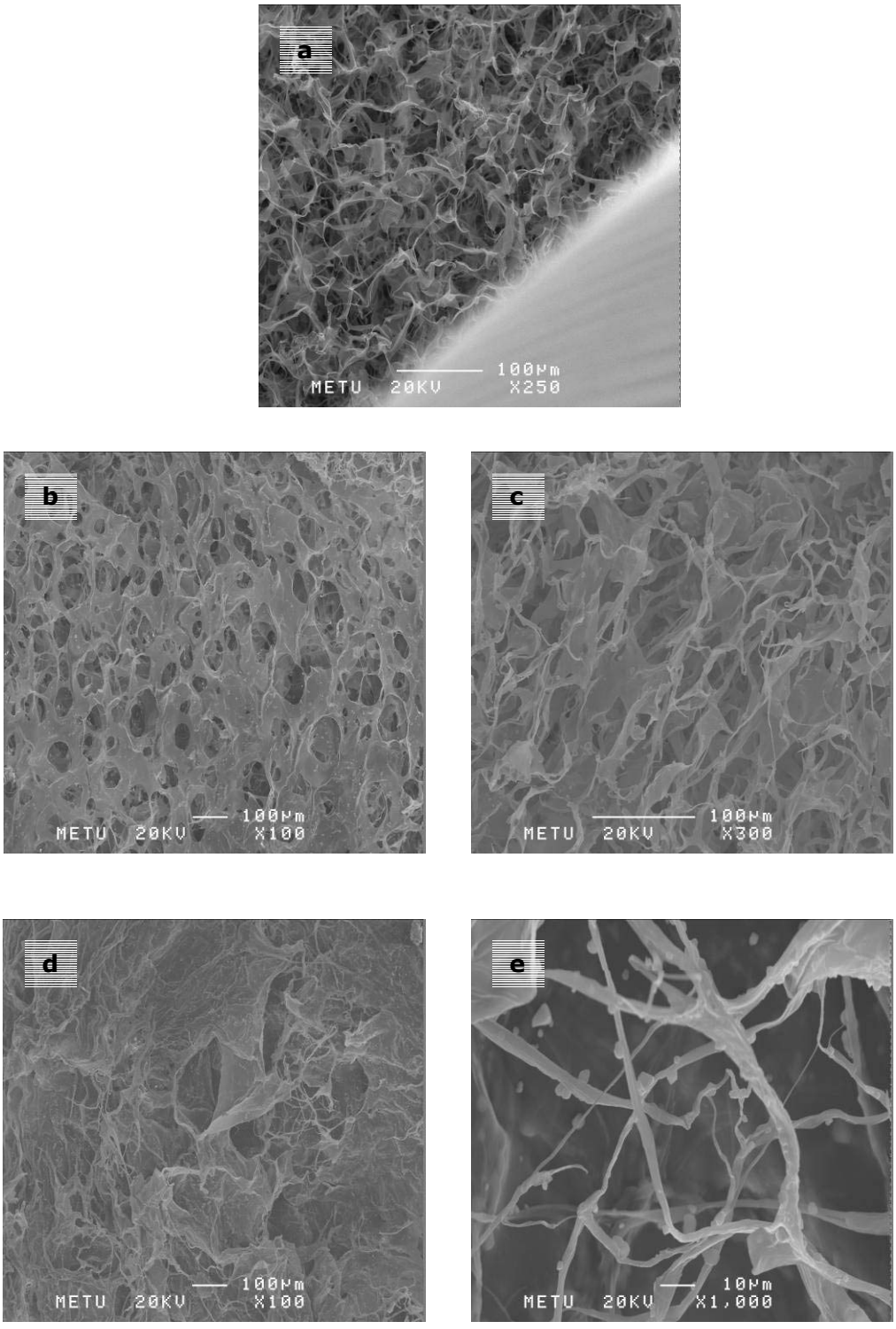

Figure 3.9 SEM micrographs of rat tail collagen foam. **a)** Week 0, **b)** Week 2, **c)** Week 4, **d)** Week 2 higher magnification, **e)** Week 4 higher magnification.

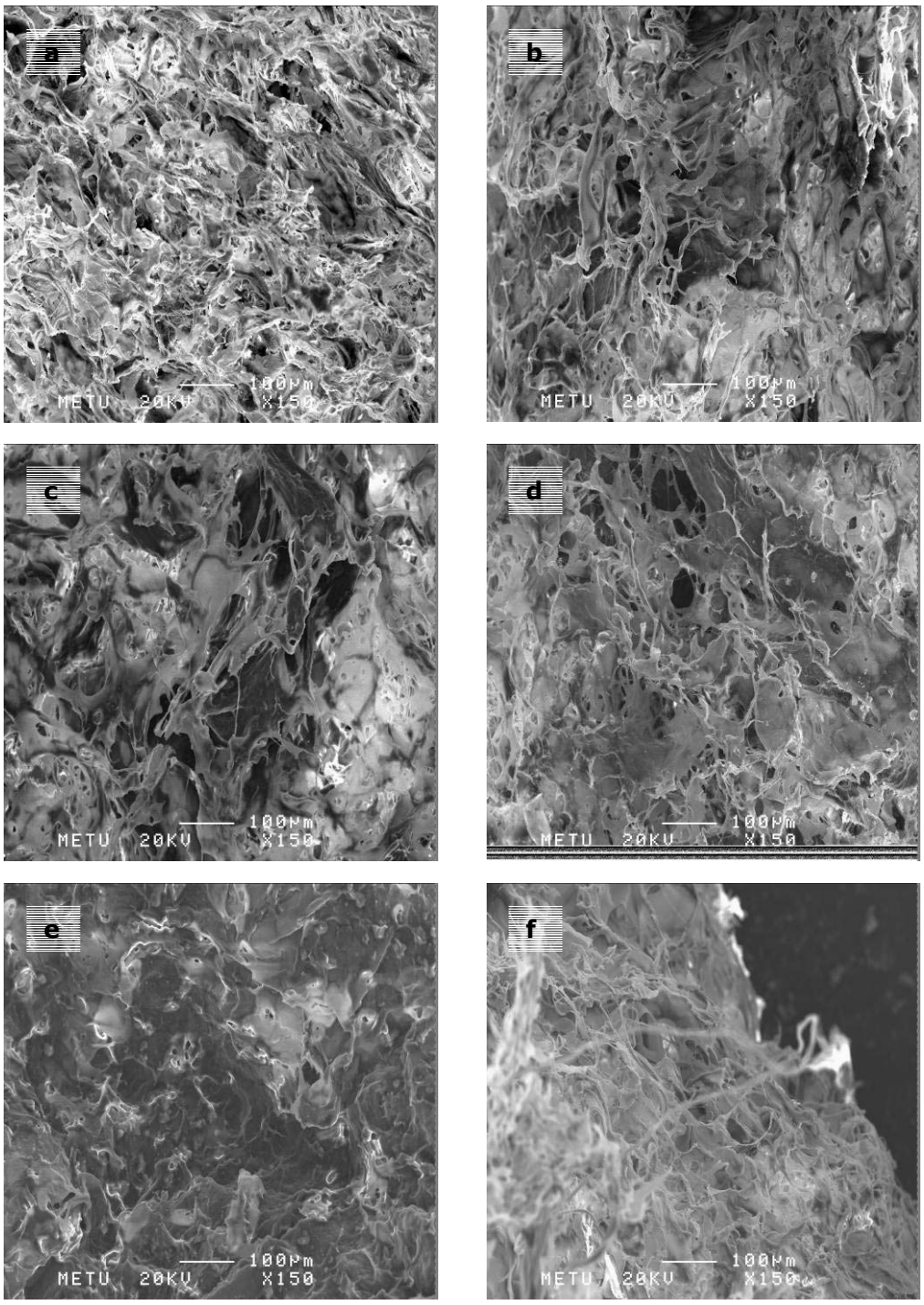

Figure 3.10 SEM micrographs of insoluble collagen foams; top surface and cross-section respectively **a, b)** Week 0, **c, d)** Week 1, **e, f)** Week 4.

3.2.1 Collagenase Susceptibility of Rat Tail Collagen Films

Another contributor to the degradation of collagen based biomaterials is the proteolytic enzymes secreted by the cells. Collageneous implants are rapidly turned over by the body through enzymatic cleavage with metalloproteinases and cathepsins (Bailey, 2000). Secretion of proteolytic metalloproteinases by corneal keratocytes is a known fact and it has been shown that nearly 20% of a collagen gel can be degraded by proteolytic actions of keratocytes (Lu et al, 2006). Thus, it is quite important to know the resistance of a collagen based scaffold to proteolytic enzymes; if resistance were too low, scaffolds would degrade before ECM secretion by the cells compensates for the lost parts. In order to test the stability of crosslinked films in the presence of an proteolytic enzyme, films were treated with collagenase for 3 h. There was a steady degradation for 3 h but crosslinked films retained their shape and resisted degradation, in contrast to uncrosslinked films which degraded immediately in the presence of collagenase (in 10 minutes). Control samples which were incubated under the same conditions but without collagenase showed no degradation demonstrating that the contribution of *in situ* degradation during this interval was negligible (Figure 3.11). Related experiments in the literature have shown similar trends; a steady degradation over time which was dependent on the initial crosslinker concentration, crosslinking duration and the activity of the collagenase utilized (Ma et al, 2004; Yao et al, 2006).

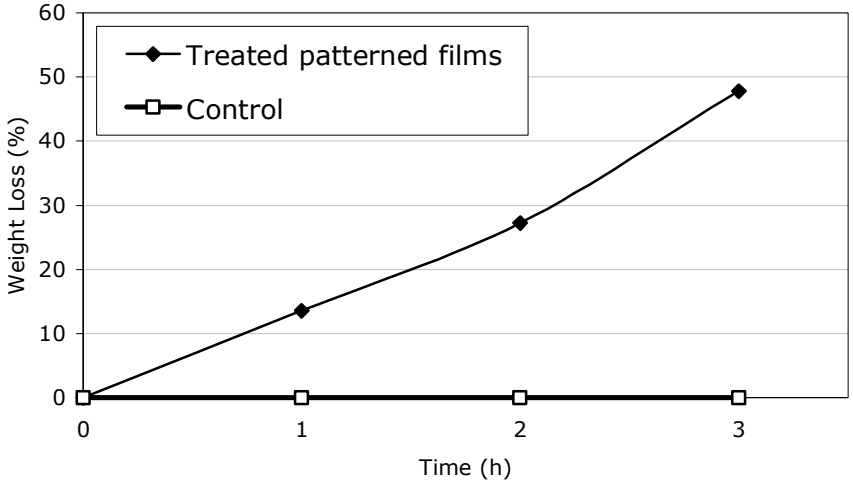

Figure 3.11 Collagenase degradation of patterned collagen films in the presence of 0.1 mg/ml(45 units) collagenase A solution in PBS (pH 7.4 , 10 mM) at 37 °C.

3.3 Cell Proliferation

Cell proliferation was determined with the MTS assay. In order to be able to determine the cell growth rate accurately, a small initial number of cells (1 x 10^4) was chosen. For films the number of cells reached 1.76 x10^5 in 10 days, an increase of 18 fold (Figure 3.12). This might be close to the limit for the cell number on collagen films (confluency) since in tissue culture flasks when confluent there are around 1.6x10^5 cells/cm^2. Due to the presence of patterns, the film structure is not exactly two dimensional and the presence of the patterns increases the overall surface area. With a higher seeding density to observe the relation between the increase in mechanical strength and cell number, 2.60x10^5 cells were reached after a period of 3 weeks (Figure 3.13). This higher number can be attributed to the faster proliferation in the beginning leading to a more excessive ECM secretion which provides more surface for cells thus increasing the available area, which was also observed by fluorescence microscopy.

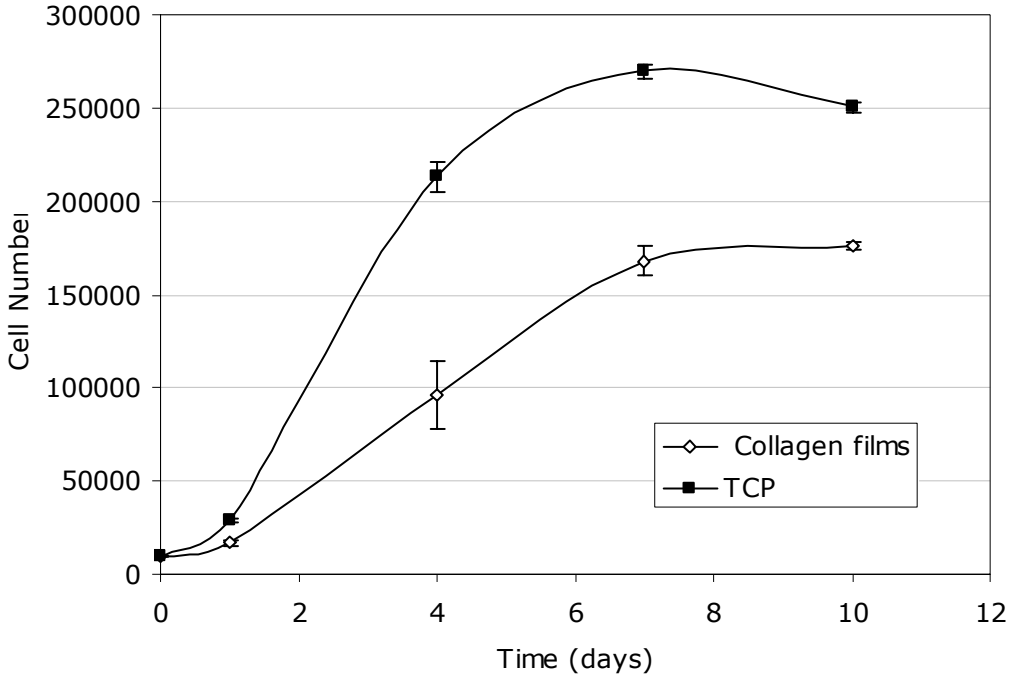

Figure 3.12 Proliferation of keratocytes on patterned collagen films. (Initial seeding number per sample 1 x 10^4)

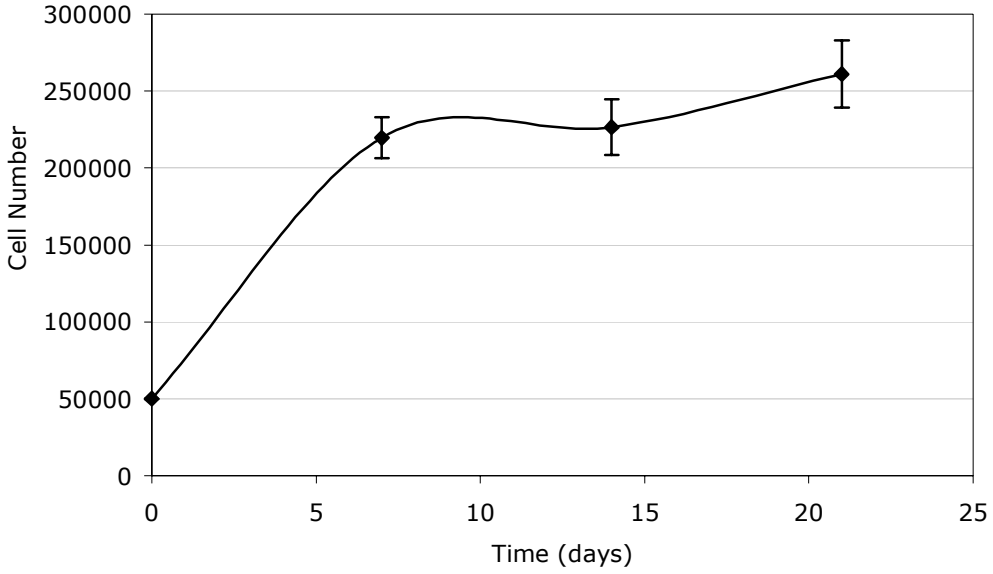

Figure 3.13 Proliferation of keratocytes on patterned collagen films in a 3 weeks period. (Initial seeding number per sample: 5 x 10^4)

In Figure 3.14, it is observed that cell number on TCP was 3.0 x 10^5 ± 2.3 x 10^3 on day 10. A single well of a 24-well of a TCP has an area of 2.54 cm^2 and the density of cells at confluency in this well is 1.6x10^5 cells/cm^2 as found by cell counter. Thus, in a well at confluency 4 x10^5 cells should be found. This number is slightly higher than the MTS results, however MTS results are in agreement with that obtained in previous studies where with a similar growth curve, the cell number per well was found to be around 3x10^5 at the end of one week (Pancholi et al, 1998). For foams, cell numbers reached on day 10 were 2.8 x 10^5 ± 1.2 x 10^4 and 2.0 x 10^5 ± 4.8 x 10^3 for rat tail collagen and insoluble collagen foams, respectively. In another study, with bovine hide collagen sponges, cell number after a 10 day period was around 4 x10^5 cell per foam, even though these foams were thicker than the one used in these experiments (thickness 1.2 mm compared to 0.532 mm and 0.811 mm respectively; Orwel et al, 2003). Foams can be expected to accommodate higher numbers of cells; however, their low thicknesses restricts the available volume for cell attachment and proliferation. Also a 50% surface porosity may cause a lag in penetration of the cells and an overall obstacle to the transport of nutrients and oxygen.

Another possible explanation is the inadequacy of the MTS assay due to the rapid utilization of the chemical which makes it difficult the accurately calculate the number of cells at high cell concentrations. What can be concluded from the data above is that RT foams are more conducive for cell growth, most probably mainly due to easier transport of oxygen and nutrients due to the less concentrated nature of the foam.

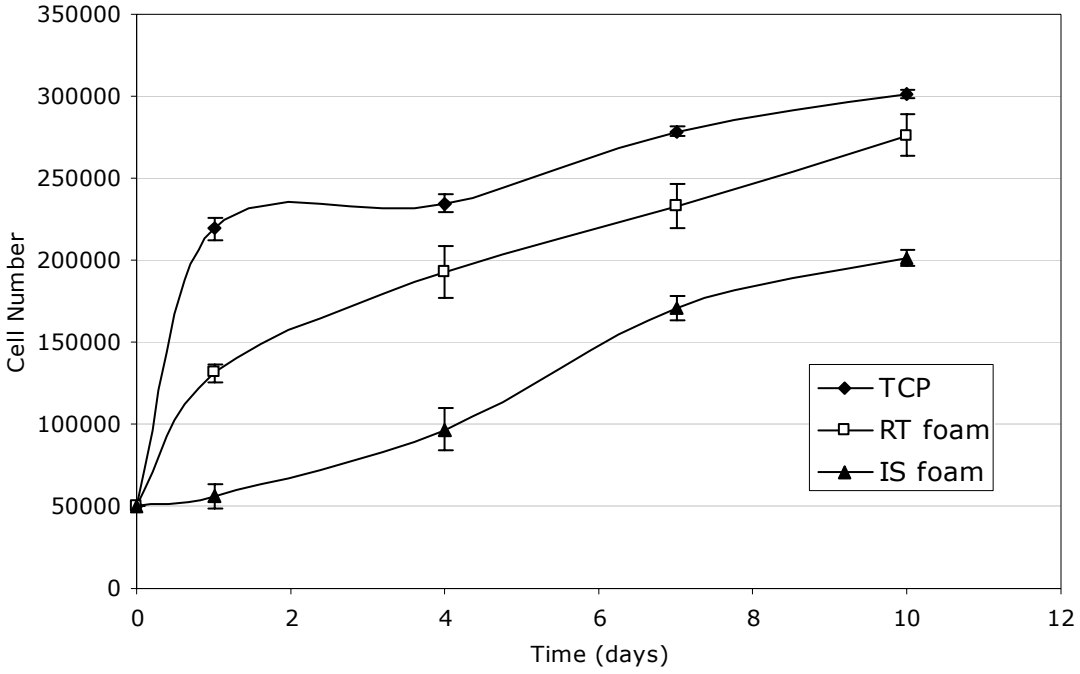

Figure 3.14 Proliferation profiles for insoluble and rat tail collagen foams (Initial seeding number per sample 5 x 10^4).

3.4 Microscopy Studies

3.4.1 Cell Morphology

Keratocytes strongly responded to surface patterns and from Day 1 they aligned in the direction of the grooves (Figure 3.15 a, b). After 7 days, cell proliferation was apparent and the cells were nearly confluent on the patterned film surface (3.15 c, d). Alignment was not lost during this period. In unpatterned films no observable anisotropy existed by day 7, but cells covered the surface in an even distribution and had a morphology quite similar to the cells grown in tissue culture flasks (Figure 3.15 e, f).

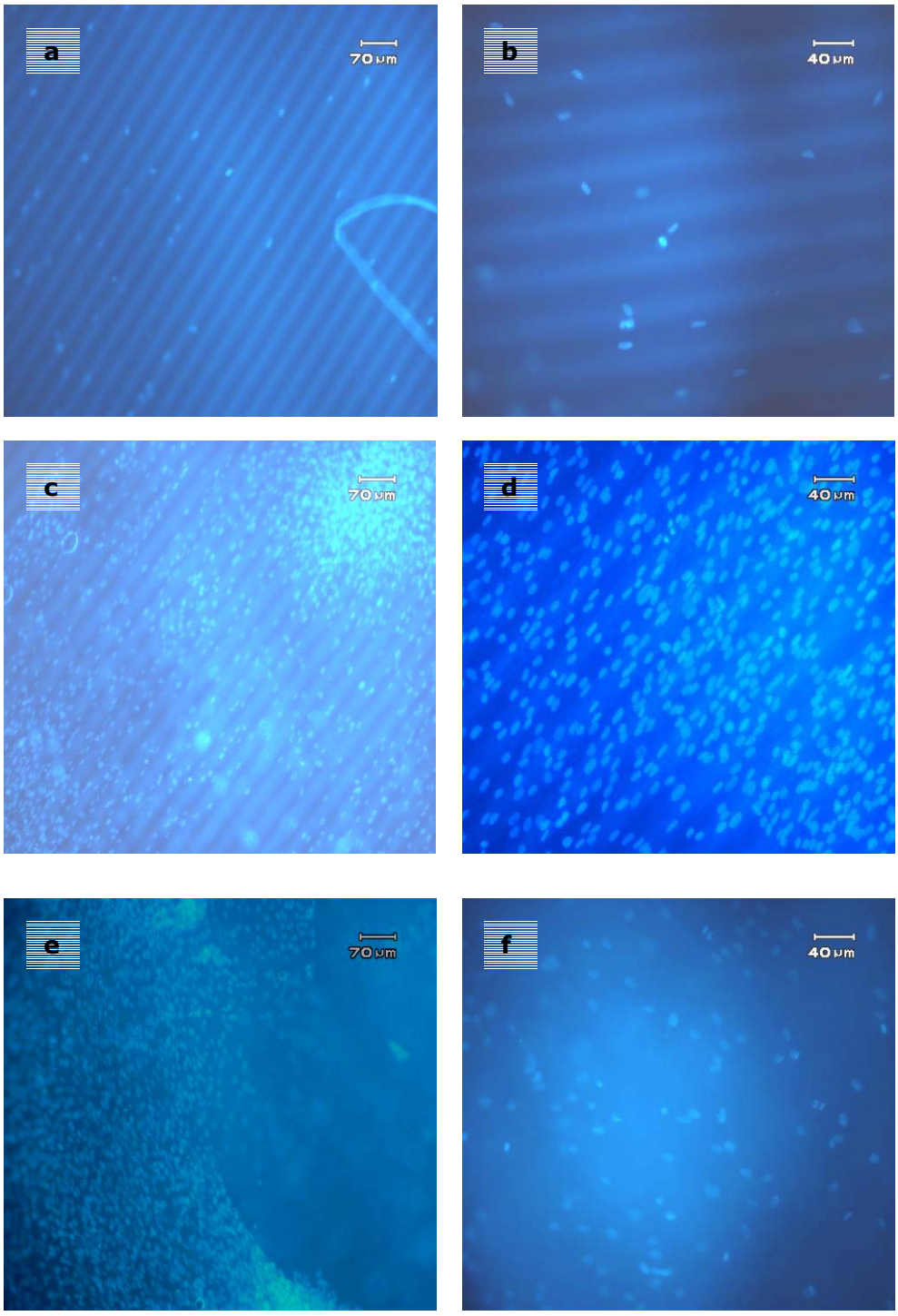

Figure 3.15 Fluorescence micrographs of DAPI stained human corneal keratocytes on: **a, b)** Patterned collagen films after 1 day of incubation, **c, d)** Patterned collagen films after 7 days of incubation, **e f)** Unpatterned collagen films after 7 days of incubation.

Loss of alignment was observed in some parts of the films but even after 21 days of culture alignment still persisted (Figure 3.16 a-d).

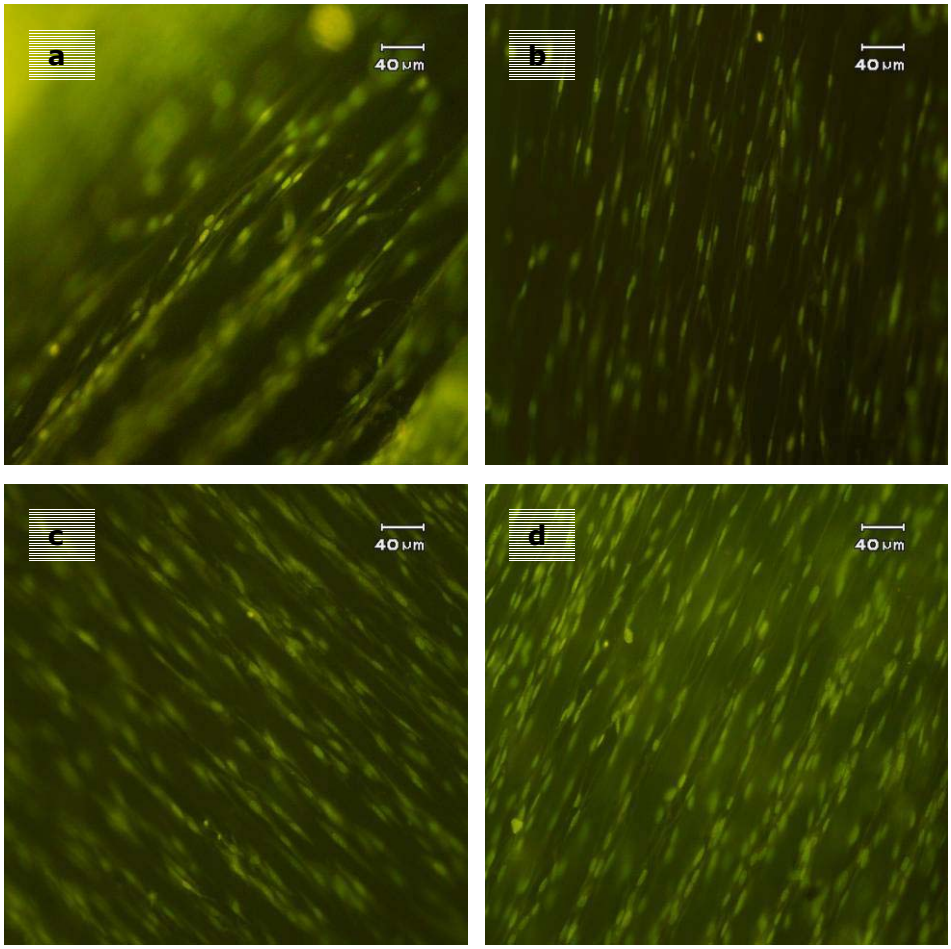

Figure 3.16 Fluorescence micrographs of Acridine orange stained human corneal keratocytes on patterned collagen films after **a)** 1 day, **b)** 7 days, **c)** 14 days, **d)** 21 days of incubation.

Some cells seemed to migrate out of the grooves and appeared out of focus since they were at higher elevations than most cells. Cells could both grow and move on the inclined surfaces of the groove and the second reason for such behavior could be the excessive secretion of ECM molecules as a response to the presence of the patterns, filling up the grooves and allowing cells to occupy positions higher than the patterns would normally allow. SEM micrographs supported this explanation. They showed individual cells on day 7 (Figure 3.17a, b), but by day 14 single cells can not be discerned and the surface had a more

amorphous appearance. This was due to the ECM secreted by the existing cells affecting the sharpness of the pattern (Figure 3.18c, d).

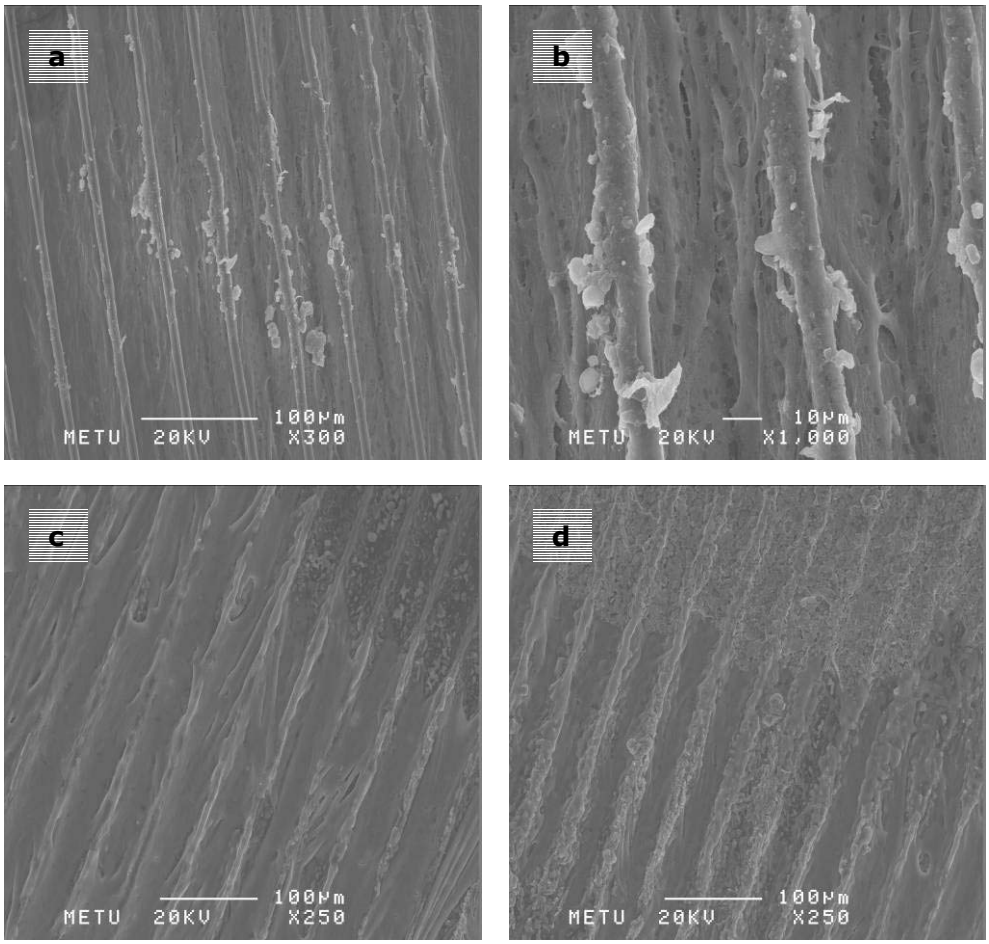

Figure 3.17 SEM micrographs of human corneal keratocytes on patterned collagen films after **a, b)** 7 days, **c, d)** 14 days of incubation.

For D407 cells which were used as a reference for mechanical tests, the response to the surface patterns was different. Cells conformed to the surface patterns but this was not as significant as that of the keratocytes. Growth of cells was slower and cells were not confluent on day 7 (Figure 3.18a). However cellular connections were quite apparent and SEM micrographs on 10 day specimens showed layers of cells on the film surface with cellular protrusions extending in the direction of the grooves (3.18 b; 3.19 a, b).

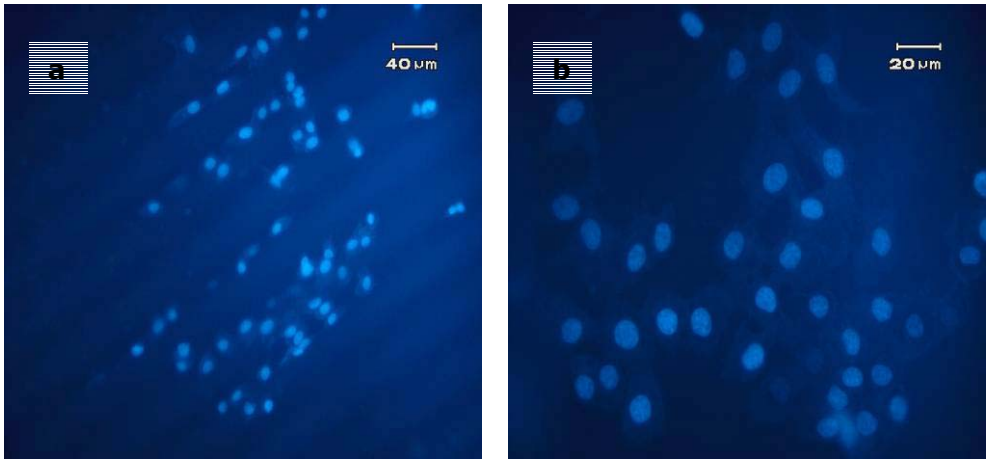

Figure 3.18 Fluorescence micrograph of D407 cells on patterned collagen films stained with DAPI after **a, b)** 7 days of incubation.

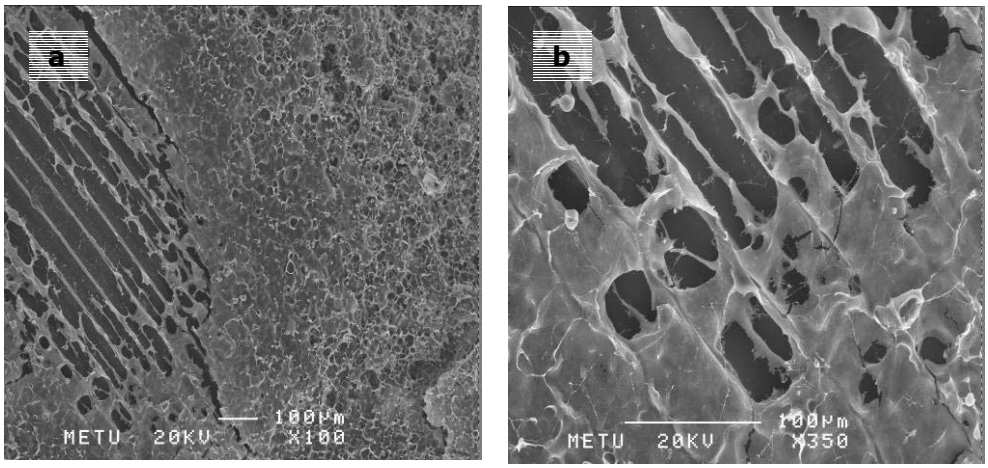

Figure 3.19 SEM micrographs of D407 cells on patterned collagen films after **(a, b)** 7 days of incubation. Magnification a) x100 b) x350

SEM micrographs of the insoluble collagen foams seeded with keratocytes showed a significant amount of spread cells on the foam surface on day 4 (Figure 3.20 a-c). Acridine orange staining for insoluble collagen foams did not produce discernible images but for rat tail collagen foams, Acridine orange staining showed cells all over the foam surface and moreover penetration of some cells (Figure 3.21a, b).

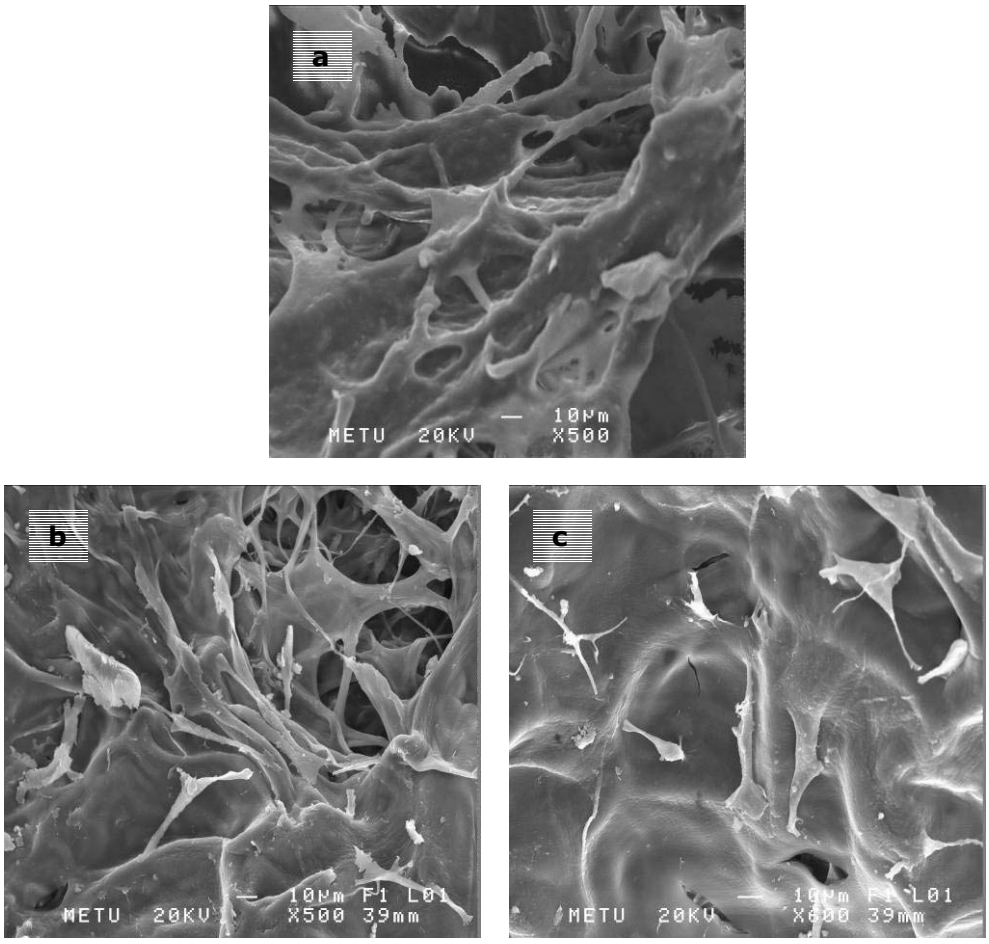

Figure 3.20 Human corneal keratocytes on insoluble collagen foams on a) Day 0 (no cells), b-c) Day 4 of incubation.

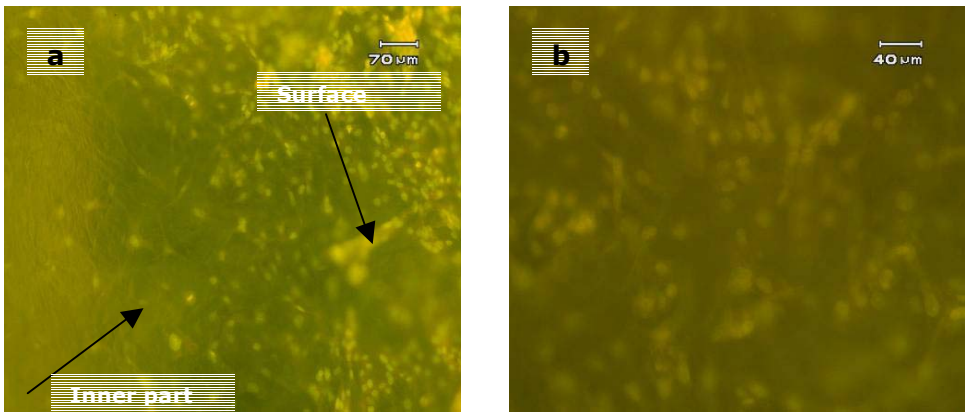

Figure 3.21 Fluorescence micrographs of keratocytes on rat tail collagen foams stained with Acridine orange after 14 days of incubation a) surface b) Close-up of the interior part.

3.4.2 Phalloidin Staining

In order to study the effect of surface patterns on the orientation of the cytoskeleton, actin fibers of the keratocytes were stained with FITC labeled Phalloidin. This showed that the orientation of cells dictated by the surface patterns also led to an increased orientation of the cytoskeleton (Figure 3.22).

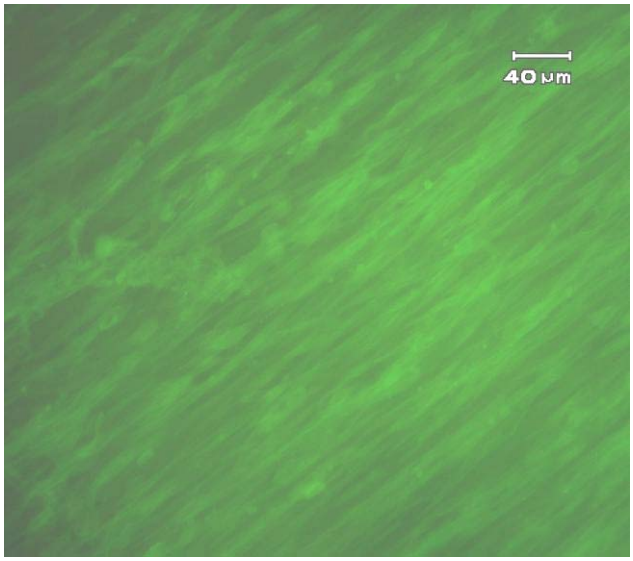

Figure 3.22 Human corneal keratocytes on patterned collagen films stained with FITC-labelled Phalloidin after 7 days of incubation.

3.4.3 Immunostaining

3.4.3.1 Collagen Type I Staining

Collagen type I is the main component of corneal stroma and its secretion is one of the main functions of the keratocytes. In order to study the effect of surface patterns on the orientation of the collagen secreted; immunostaining was carried out. In the beginning, the expectation was to have a significant background because the scaffolds themselves were also composed of collagen type I that would react with the antibody used. However background stain was insignificant; most probably due to the modification of the epitope recognized by the antibody during crosslinking (Figure 3.23a). This made the examination of the secreted collagen easier.

On the first day of incubation; the immunolabeling was mainly concentrated at certain locations which were occupied by the cells. Cell structure was quite apparent because most of the collagen labeled was within the cell cytosol (Figure 3.23 b). After 7 days of incubation secreted collagen fibers can be seen like an ECM structure and secretion was in the direction of the grooves (Figure 3.23 c). Collagen secretion by D407 cells(the control) was practically non-existent on Day 7 (Figure 3.23d). However, secreted collagen did not appear to be fibrillar over the whole surface. Collagen secretion by D407 cells(the control) was practically non-existent on Day 7 (Figure 3.23d).

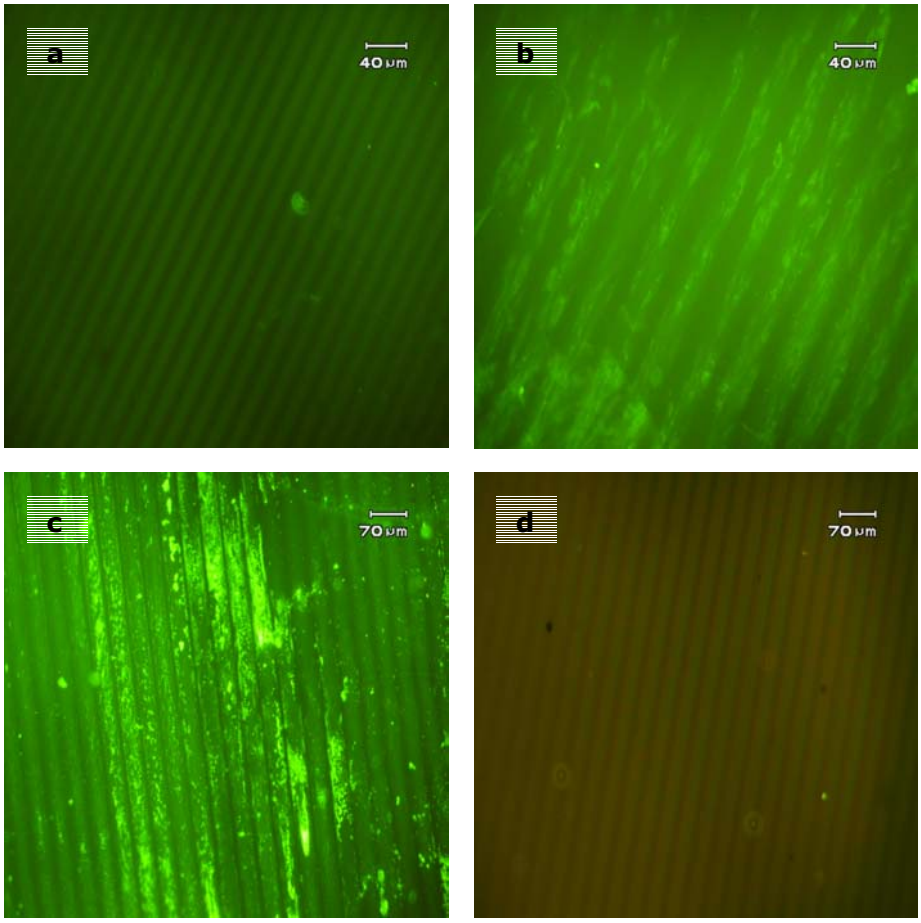

Figure 3.23 Immunolabeling of secreted collagen type I by human corneal keratocytes (b,c) and D407 cells (d) on patterned collagen films. **a)** Control, **b)** Day 1 of incubation, **c)** Day 7 of incubation **d)** Day 7 of incubation for D407 seeded films .

In the keratocyte seeded unpatterned film samples, collagen secretion seemed to be less with respect to the patterned counterparts and as expected there was no sign of anisotropy (Figure 3.24).

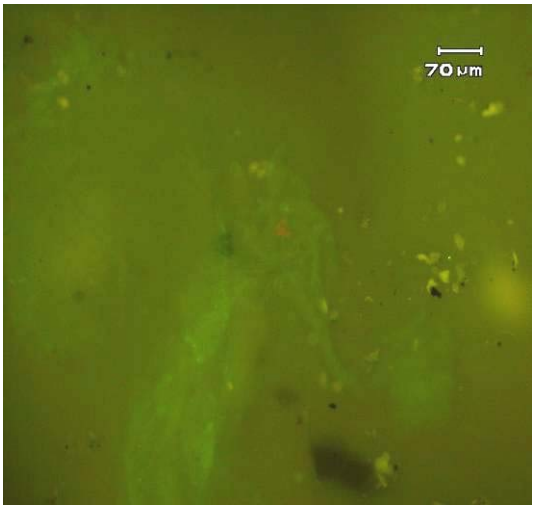

Figure 3.24 Immunostaining of collagen type I secreted by keratocytes on unpatterned collagen films after 7 days of incubation.

3.4.3.2 Keratan Sulfate Staining

Keratan sulfate is a glycosaminoglycan and is an essential component of the corneal stroma structure. It is found in three corneal proteoglycans (lumican, keratocan and mimecan) and is responsible of the hydration of the stroma and the orientation of the collagen fibers (Funderburgh et al, 2003). Thus it contributes to corneal transparency. These proteoglycans are quite oriented, surrounding the individual collagen fibers. They are also secreted by the keratocytes and their presence is an indicator of the proper keratocyte behavior (Funderburgh, 2000). Hence, both patterned and unpatterned films were seeded with keratocytes and stained for keratan sulfate secretion. Secretion was observed in both specimens on Day 1 and Day 7 (Figure 3.25a-d). As with collagen type I, secretion conformed to the patterns of the films but there was no orientation in unpatterned ones.

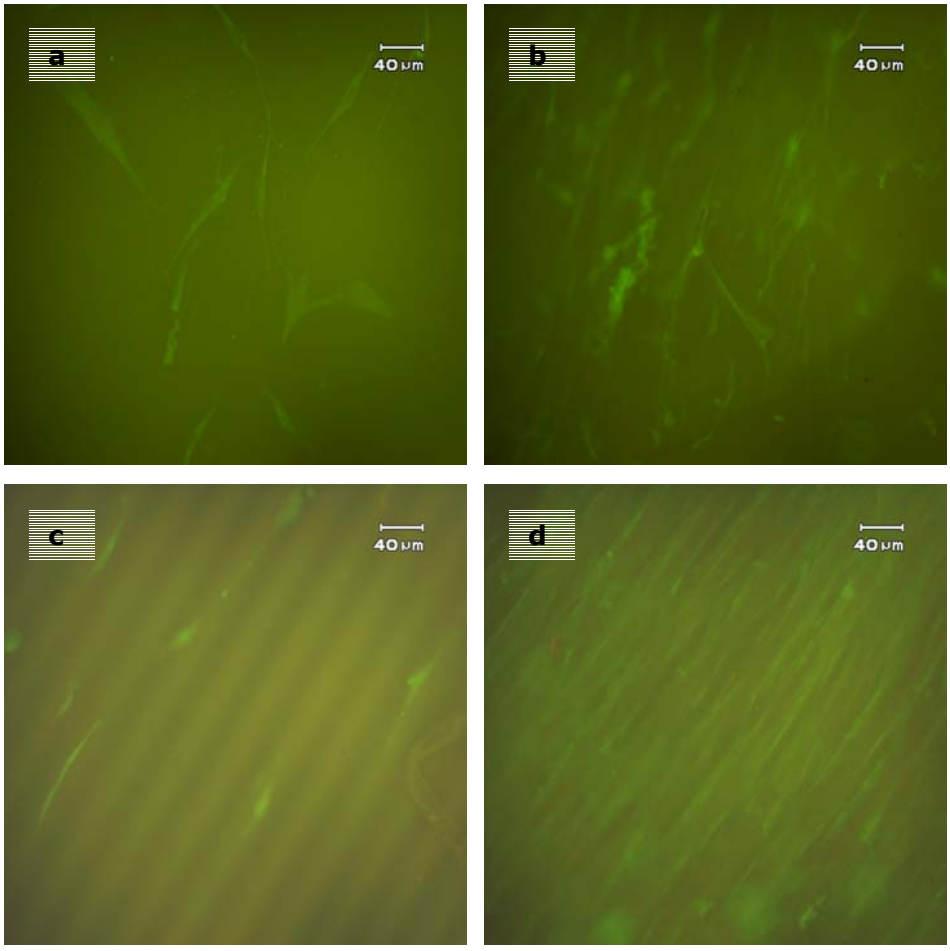

Figure 3.25 Keratan sulfate staining for keratocytes seeded on **a-b)** unpatterned Day 1 and Day 7, **c-d)** Patterned films Day 1 and Day 7 samples, respectively.

3.4.4 Confocal Microscopy (CLSM)

Confocal studies were carried out to study the mobility of the cells and obtain proof of penetration into the foams and also to see the distribution of the secreted collagen. Confocal images of RT foams showed spread cells within the 100 micrometer depth of the scaffolds (Figure 3.26 a,b).

Spread cells were also observed within the insoluble collagen foams, the cross-sections revealed that cells have moved to the edges; but not in a homogenous manner (Figure 3.27 a-c)

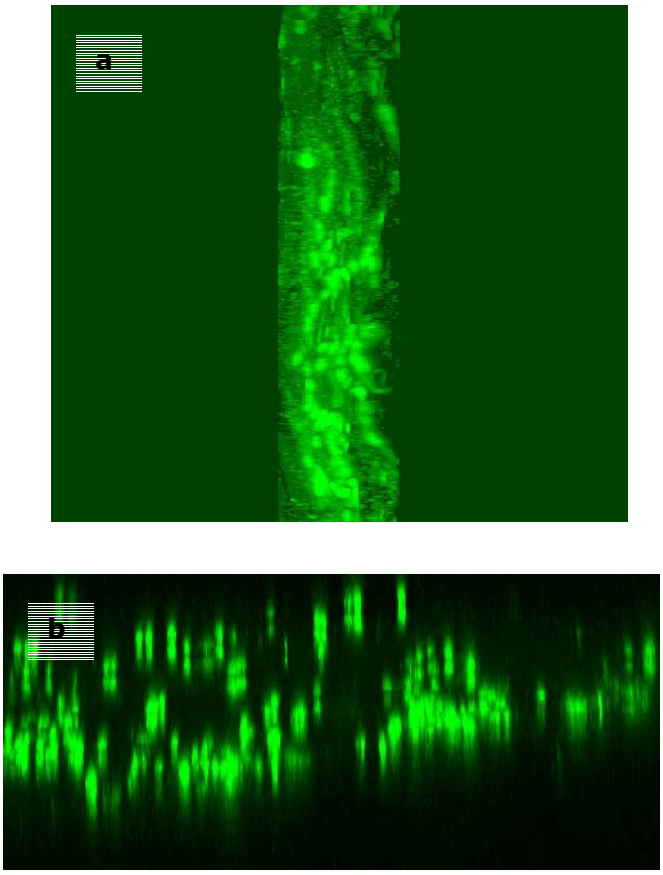

Figure 3.26 CLSM images of Acridine orange stained keratocyte seeded rat tail collagen foams after 15 days **a)** Distribution of spread cells inside the foam; cells were seeded from the right hand side (Magnification x40) **b)** Distribution of the keratocytes in lateral direction and penetration of the cells inside the foam, thickness 100 µm; cells were seeded from the top (Magnification x10).

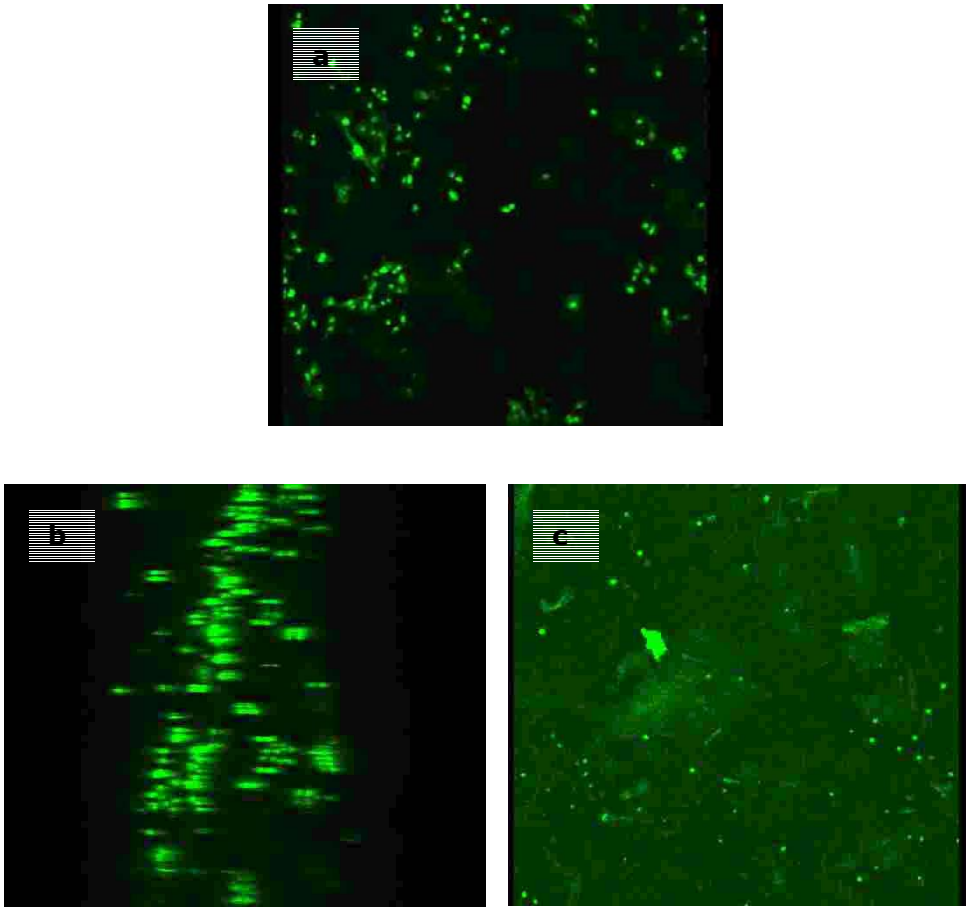

Figure 3.27 CLSM images of Acridine orange stained keratocyte seeded Insoluble collagen foams on after 10 days: **a)** Top view for cell distribution on the surface (Magnification x20), **b)** Cell penetration into the foams; cells were seeded from the left hand side (Magnification x20), **c)** Lateral cell distribution on a cross-section (Magnification x10).

When investigated by CLSM, collagen secretion by the keratocytes was seen not to be homogenously distributed on the patterned films and also most of the secretion was localized in the base of the grooves (Figure 3.28a, b).

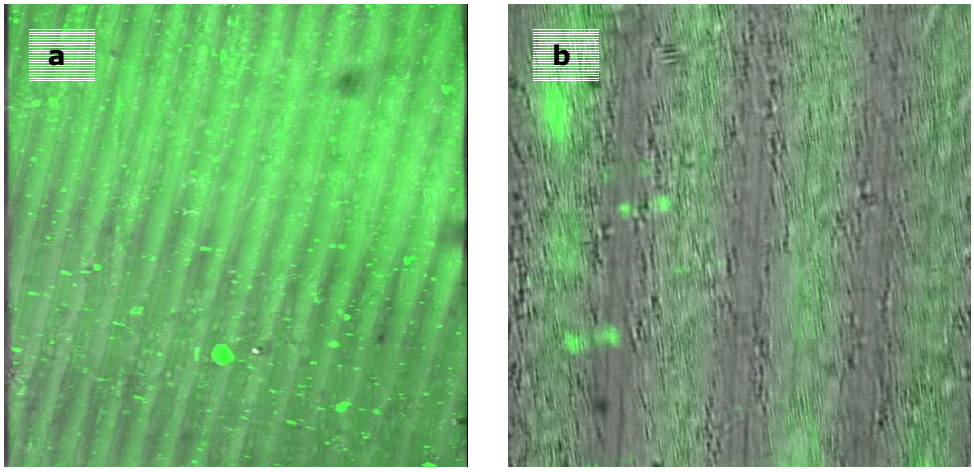

Figure 3.28 Confocal images of collagen type I immunostaining after 7 days of incubation. Magnification **a)** x 10, **b)** x 40 focused on the base of the grooves.

3.5 Mechanical tests

Cornea withstands the shear forces exerted by the tear film and by the eyelids and also ensures the constant inner hydrodynamic pressure. To this end, the structure of the corneal stroma is important and any attempt to simulate corneal stroma should take into account this property. As described earlier, patterned collagen films are quite good at orienting cells and ECM materials; but they were susceptible to collagenase activity and were also shown to degrade through erosion as shown by the *in situ* degradation experiments (Section 3.4). Thus, the mechanical strength of the films, in the presence and absence of the cells, was quite important and in order to see the effect of the cell type, D407 cells were used as a reference, a model epithelial layer. There were three groups of specimens: a) unseeded films, b) films seeded with keratocytes and c) films seeded with D407 cells. These samples were incubated for time periods of 1, 2 and 3 weeks in the cell culture and their tensile strength was determined.

The mechanical strength of the unseeded samples decreased significantly after the first week, followed by less prominent decreases in the following weeks (Figure 3.29a). This correlates well with the leveling out of the degradation after two weeks. The only thing that should be considered while doing such a comparison was the presence of the serum proteins that can get absorbed onto

the degradation samples in this experiment and contribute to the overall mechanical strength of the system, which were totally absent in the in-situ degradation experiments. As can be seen from the graphs there was a sudden decrease in the ultimate strength (strength at failure) in the first week. In the following weeks, this decrease in the ultimate strength was not so significant but there was an increase in the strain at failure. This in general pointed out a decrease of stiffness of the scaffold which would be expected with the loss of material from the scaffold. For specimens seeded with keratocytes ; the increase in the ultimate strength in the first week was around 33% of the original strength which was quite significant. This was followed by smaller increases in the stiffness of the scaffolds in the following weeks (Figure 3.29 b). The final increase of ultimate strength was more than 50% of the initial strength without any significant changes in the final strain which means that the scaffolds in the presence of the keratocytes have become stiffer. For epithelial cell seeded specimens a 25% decrease in ultimate strength was observed after 1 week period; followed by a small improvement in the subsequent weeks which was only about 10% of the initial strength (Figure 3.29c).

a)

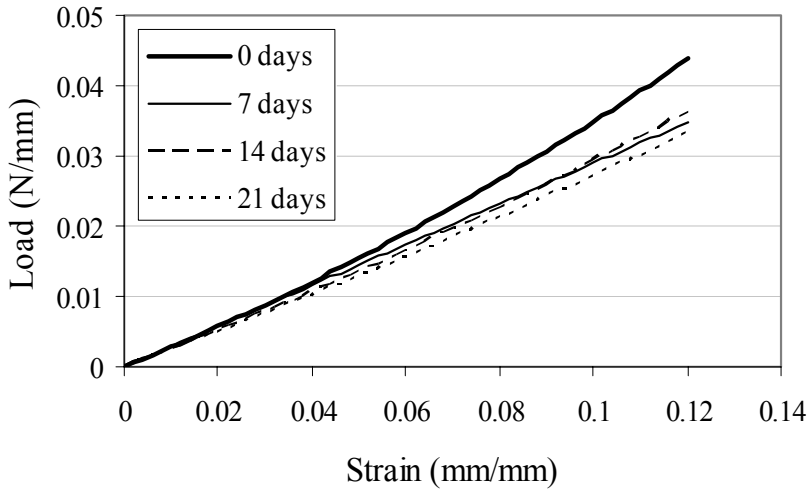

b)

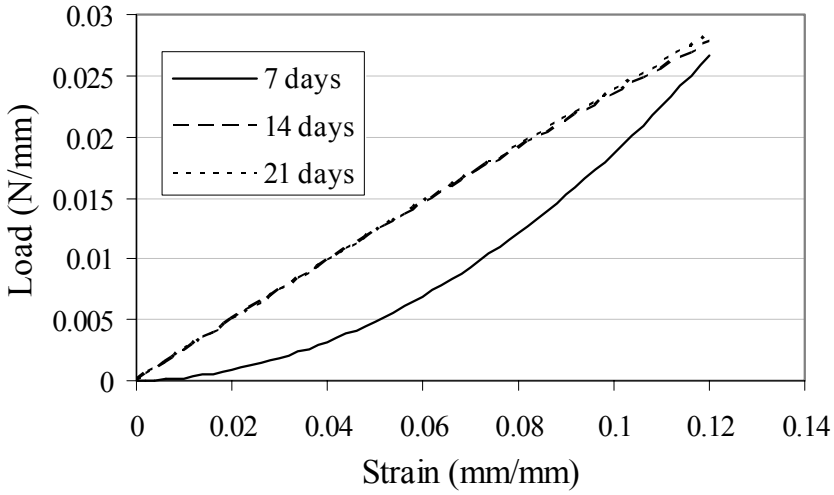

c)

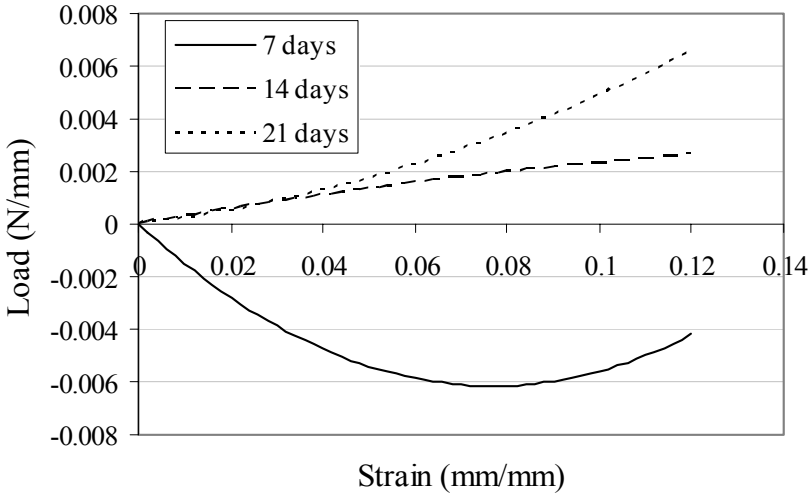

Figure 3.29 Mechanical test results of patterned rat tail collagen films. **a)** Load vs. strain curve for unseeded films over a 21 day period, **b)** Performance of keratocyte seeded patterned collagen films with respect to reference films (Relative to day 0; day 0 data was subtracted from data obtained on days 7,14 and 21), **c)** Performance of D407 seeded patterned collagen films with respect to the reference films (Normalized with respect to day 0).

This behavior can be related to several effects. First, previous experiments with D407 cells and keratocytes have shown a better conformation to the pattern by keratocytes. This would create the anisotropy necessary to

create an improvement in tensile strength in that axis, since loading was parallel to the groove direction. Also D407 cells were lower in number by day 7; so this might be another factor. The smaller increase in weeks 2 and 3 can be related to the decreasing rate of cell growth confirmed by the MTS results. The patterned surface would help the increase in tensile strength in the direction parallel to the patterns, since it would provide necessary cues that would direct cell, cytoskeleton and extracellular matrix arrangement as shown by the immunolabelling above. Thus oriented collagen type I and keratan sulfate secretion would provide the necessary compensation against the activity of secreted collagenase enzymes and also degradation by erosion. The same is not true for D407 cells, since their extracellular matrix secretion is limited and they have a higher collagenase activity. Since endurance of the films to collagenase activity was not high, low cell density and insufficient ECM would not be enough to compensate the degradation of the films, which would explain the decrease in strength. However as all epithelial cells they tend to establish strong cell to cell connections which could be the reason for the rectification of the mechanical strength of the films after 2 weeks and in the long run may result in an hyperelastic behavior of the scaffolds.

3.6 Transparency Measurements

Transparency is one of the most important properties of the cornea and it should be regained for an artificial cornea implantation to be considered successful. It is, therefore important to investigate the *in vitro* transparency for any artificial cornea product. In order to study this, patterned and unpatterned films seeded with keratocytes and cell-free patterned films were tested for their transparency of light in the UV-VIS range over 7 days. In addition to films, foams seeded with keratocytes were also tested for their transparency after one week.

Initially patterned and unpatterned films have a 30% percent transmittance of the incoming visible light, with unpatterned films being slightly more transparent (Figure 3.30 a). Transparency of the unseeded patterned films increased and at the 7^{th} day reached about 40 % (Figure 3.30 b-d). Patterned collagen films seeded with keratocytes showed a consistent transparency over this period after an initial slight decline (Figure 3.30 b-d). On the other hand,

unpatterned collagen films seeded with keratocyte encountered a significant decline of transparency followed by a recovery over a one week period (Figure 3.30 b-d).

Increase of transparency due to degradation can mainly be attributed to the decrease in thickness of the films during degradation. This would be countered by the deterioration of the surface which would increase the scattering, though degradation experiments showed that erosion was not too significant during this period. For cell seeded films, the decrease in transparency was expected; patterns align cells and also their secreted products or the aligned cytoskeleton triggers aligned ECM deposition. Since this was not the case for unpatterned films, the disorganized distribution of the cells and ECM would instead increase the scattering of the light and decrease transparency. But degradation and remodeling by the proliferating keratocytes helped increase transparency. Despite the increase in transparency for unpatterned films following the initial decrease, patterned films still had a better performance, probably because the organization achieved on the patterned films was quite effective.

a)

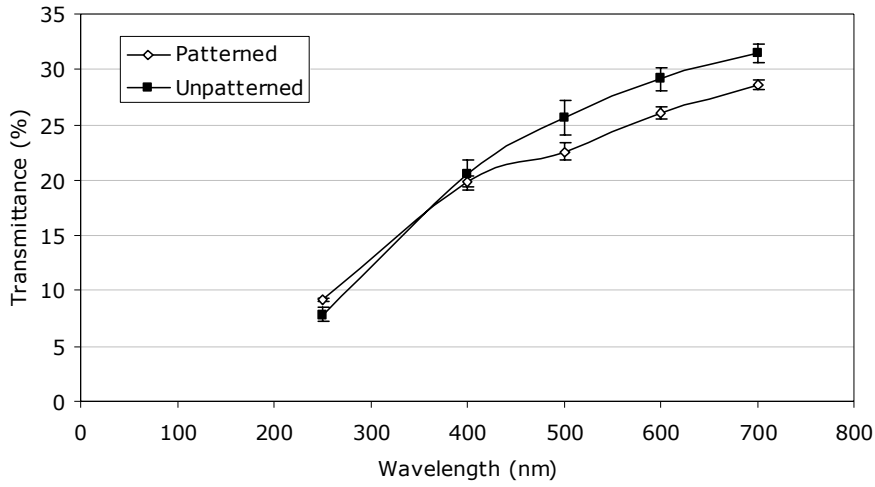

b)

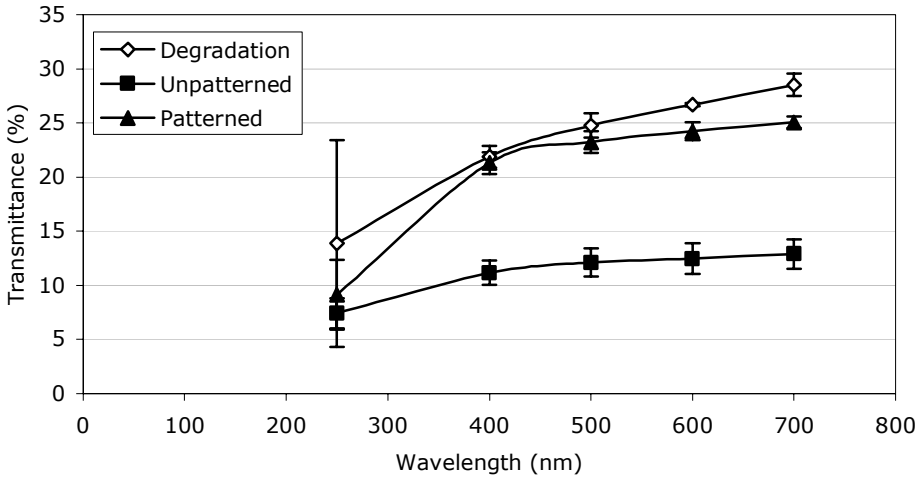

c)

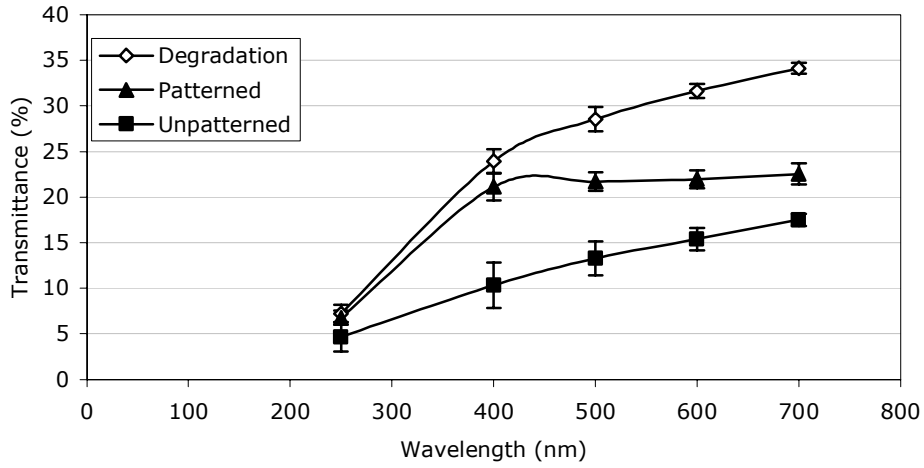

d)

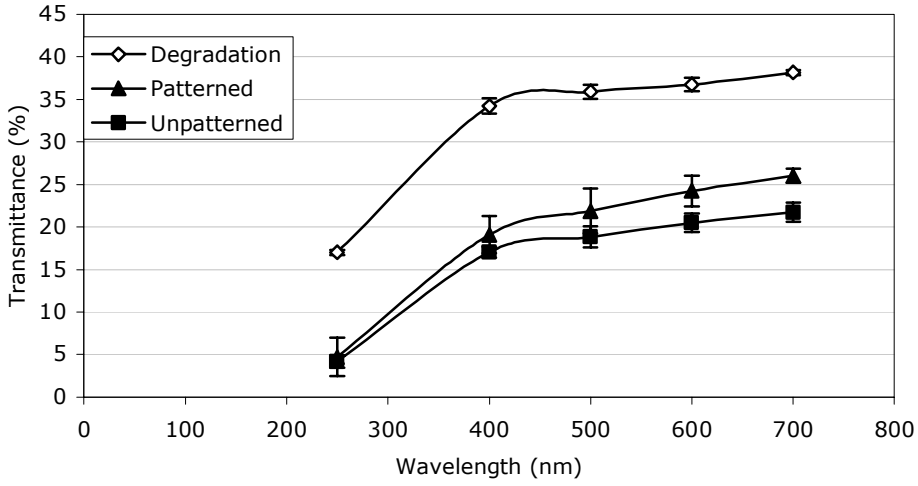

Figure 3.30 Transparency of collagen films. **a)** Transparency of patterned and unpatterned films on Day 0; Transparency of unseeded patterned ("degradation"), keratocyte seeded patterned, and keratocyte seeded unpatterned films on **b)** Day1, **c)** Day4, **d)** Day7.

For the foams, remodeling was slower, thus the transparency change was minimal. In a one week period, transparency of the rat tail collagen foams increased to 4% from being totally opaque. The change was practically zero for insoluble collagen foams (Table 3.5). The thickness and the amount of unorganized collagen present were the reasons for such behavior. But the increase in transparency in RT foams indicates that cellular activity and degradation can lead to increase in transparency in a longer culture period.

Table 3.5. Transparency of foams (% Transmission)

Wavelength (nm)	**Type**					
	Rat Tail			**Insoluble**		
	Day 0	Day 7 Seeded	Day 7 Unseeded	Day 0	Day 7 Seeded	Day 7 Unseeded
700	0	3.70	5.61	0	0.54	0.50
600	0	3.25	5.08	0	0.47	0.46
500	0	2.71	5.03	0	0.41	0.42
400	0	2.04	4.11	0	0.30	0.36
250	0	0.28	0.99	0	0.07	0.14

CHAPTER 4

CONCLUSION

A tissue engineered cornea must satisfy several requirements. It should be biodegradable, should have a certain thickness, must be conducive to the proliferation of corneal cells, should be strong enough to withstand intraocular pressure and other forces exerted on the natural cornea, and it must be transparent. In this study, collagen was selected as the scaffold material, since it is one of the major constituents of the natural cornea and also as a natural polymer it is biodegradable and biocompatible. In this study 3 scaffolds were produced, insoluble collagen foams, rat tail collagen foams, and micropatterned rat tail collagen films using 2 different collagen sources, insoluble collagen from bovine trachea, and rat tail collagen.

Foams are very appropriate structures for cornea reconstruction; they are highly porous, thus they permit cell penetration and also allow transfer of nutrients and wastes. Physical characterization of both of these foams showed that bulk porosity and average pore size of these foams are appropriate for cellular penetration. A skin layer was however observed in insoluble collagen foams formed during the freeze-drying procedure. Another problem associated with the collagen foams was the preservation of the initial thickness of the foams following stabilization (e.g. crosslinking) procedures. This was not very significant with insoluble collagen foams, for which shrinkage was not extensive. Rat tail collagen foams, however, lost their porosity and thickness following the conventional crosslinking procedure. Thus, a novel crosslinking procedure was developed to maintain the thickness of these foams. With this technique, foams which have a thickness very close to that of the native cornea.

In vitro studies carried out with human corneal keratocytes demonstrated that both foams were appropriate for keratocyte growth. Quantitative studies showed that rat tail collagen foams reached a higher final cell number and density. Microscopy studies have shown that cells spread on the surface and penetrated into the interior regions of the foams.

Cornea has a very unique structure. The orientation of the collagen fibrils in the corneal stroma is essential for proper functioning of the cornea. Since transparency and mechanical properties of the cornea are dependent on this architecture, the utilization of micropatterned surfaces to guide cellular behavior and to mimic native corneal organization was deemed beneficial. Hence, possible benefits of incorporation of micropatterned surfaces in artificial cornea design were investigated by using collagen films with micro-level patterns in the form of channels with sloping sides and narrow ridges. Human corneal keratocytes grew on these patterned collagen films in a fast rate and they conformed to the surface patterns and elongated in the groove direction as confirmed by quantitative MTS assay and microscopy observations. The presence of the patterns also affected the ECM secretion and cytoskelatal orientation and these features were observed with immunostaining. These experiments showed that keratocytes on patterned collagen films secreted oriented collagen type I and keratan sulfate in contrast to unpatterned collagen films in which secretion was random.

Degradation and remodeling of the scaffolds by the cells in *in vivo* conditions is very important for the successful integration of the artificial tissue to the host. Thus, *in situ* degradation studies were carried out with both foams. Foams degraded with a steady pace without losing their structural integrity for a month. Microscopy revealed an increase in the pore size and a more disorganized appearance following degradation.

In situ degradation experiments were also done with patterned collagen films and they showed a degradation pattern similar to that of collagen foams. Surface patterns were still visible but quite deteriorated after a 1 month incubation period. In addition to these resistance of the collagen films to collagenase activity which is known to be secreted by the keratocytes during remodeling of the cornea was studied. Stabilization of the films with EDC/NHS

crosslinking increased the resistance of the films to collagenase activity significantly.

In order to see the effects of degradation and the presence of the keratocytes on the mechanical properties of the patterned collagen films, tensile strength tests were performed on unseeded films as well as on films seeded with keratocytes and with D407 epithelial cells (D407 were used as a reference for a three week period). These experiments showed that the presence of the keratocytes on the films compensated for the decrease in the strength of the carrier due to hydrolytic degradation. This was probably due to the alignment of the cells on the surface and secretion of the ECM components oriented along the pattern axis. Meanwhile, the mechanical strength of the cell-free films decreased during the experiments. Similarly, films seeded with D407 cells did not show any improvement (actually, a major loss of mechanical property was observed in the early days of incubation). These results were very promising for the suitability of collagen film scaffolds *in vivo*.

The most crucial feature of the oriented corneal stroma structure is its role in corneal transparency. Organization of collagen fibrils and proteoglycans is essential for corneal transparency. In order to see whether the organization achieved by the micropatterned films had a similar effect or not, transparency of the patterned collagen films was measured both in the presence and absence of keratocytes and compared to the transparency of unpatterned collagen films seeded with keratocytes. Transparency of unseeded films increased steadily over an one week period. Transparency of keratocyte seeded patterned films decreased slightly after seeding but stayed at the same level for the duration of the experiment. For unpatterned films seeded with keratocytes, there was a significant decrease in transparency after seeding and although transparency improved afterwards it did not reach to the level of patterned collagen films. This results demonstrated that the utilization of micropatterning is beneficial in cornea tissue engineering applications.

In this study, it was possible to prepare collagen based micropatterned scaffolds using a silicon wafer and then a silicone template, successively, starting from original designs. This led to the construction of collagen films which were able to control cell growth through contact guidance, leading to restriction of

cells and secreted ECM within the pattern grooves, resulting in a higher mechanical strength and transparency in comparison to unpatterned collagen films. Thus, the cell loaded constructs revealed a significant potential for use as total artificial corneal substitutes .

REFERENCES

Adamis A.P.,Filatov V.,Tripathi B.J.,Tripathi R.C., 1993, Fuchs' endothelial dystrophy of the cornea, Surv Ophthalmol.,38,149-68

Alberts B, Johnson A., Lewis J., Raff M., Roberts K., Walter P., 2002, Molecular Biology of the cell 4. Edition

Angele P., Abke J., Kujat R., Faltermeier H., Schumann D., Nerlich M., Kinner B., Englert C.,Ruszczak Z., Mehrl R., Mueller R., 2004, Influence of different collagen species on physico-chemical properties of crosslinked collagen matrices,Biomaterials 25, 2831–2841

Bailey A.J., 2000, The fate of collagen implants in tissue defects, Wound Rep. Reg., 8, 5-12

Bellamkonda R.V., 2006, Peripheral nerve regeneration: An opinion on channels, scaffolds and anisotropy, Biomaterials, 27, 3515-3518

Ber S., Köse G.T., Hasırcı V., 2005, Bone tissue engineering on patterned collagen films: an in vitro study, Biomaterials, 26, 1977–1986

Bianco P. ,Robey P.G, 2001, Stem cells in tissue engineering, Nature, 414, 117-121

Boyce S.T., 2004, Fabrication, quality assurance, and assessment of cultured skin substitutes for treatment of skin wounds, Biochemical Engineering Journal , 20, 107–112

Chakravarti S., Petroll W. M. , Hassell J.R. , Jester J.V., Lass J.H., Paul J., Birk D. E., 2000, Corneal Opacity in Lumican-Null Mice: Defects in Collagen Fibril Structure and Packing in the Posterior Stroma, Investigative Ophthalmology and Visual Science, 41, 3365-3373

Chalupa E, Swarbrick H.A., Holden B.A., Sjostrand J., 1987, Severe corneal infections associated with contact lens wear, Opthalmology, 94, 17-22

Chapekar M.S.,2000, Tissue Engineering: Challenges and Opportunities, J Biomed Mater. Res. (Appl. Biomater.), 53, 617–620

Chen G., Ushida T, Tateishi T., 2002, Scaffold design for tissue engineering, Macromol. Biosci., 2, 67-76

Chen R., Ho H., Sheu M., 2005, Characterization of collagen matrices crosslinked using microbial transglutaminase, Biomaterials, 26, 4229-4235

Chen V.J., Smith L.A., Ma P.X., 2006, Bone regeneration on computer-designed nano-fibrous scaffolds, Biomaterials, 27, 3973-3979

Chirilla T.,Hicks C.R., Dalton P., Sajojini V., Lou X. , Hong Y., Clayton A.B., Ziegelaar B.W., Fitton J.H., Platten S., Crawford G.J., Constable I.J., 1998, Artificial cornea,Prog. Polym. Sci., 23, 447-473

Chua C.K., Leong K.F., Cheah C.M., Chua S.M., 2003, Development of a Tissue Engineering Scaffold Structure Library for Rapid Prototyping. Part 1: Investigation and Classification, Int. J. Adv. Manuf. Technol., 21, 291–301

Claesson M., Armitage W.J., Fagerholm P., Stenevi U., 1997, Visual outcome in corneal grafts:a preliminary analysis of Swedish corneal transplant register, Br J Ophthalmol, 86, 174–180

Clark J.I., 2004, Order and disorder in the transparent media of the eye,Experimental Eye Research, 78, 427-432

Cursiefen C., Chen L., Dana M.R., Streilein J.W., 2003 Corneal lymphangiogenesis: evidence, mechanisms, and implications for corneal transplant immunology, Cornea, 22, 273-81

Curtis A.S.G., Wilkinson C., 1987, Topographical control of cells, Biomaterials, 18, 1573-1583

Daamen W.F., van Moerkerk H.Th.B., Hafmans T., Buttafoco L., Poot A.A., Veerkamp J.H., van Kuppevelt T.H., 2003, Preparation and evaluation of molecularly-defined collagen–elastin–glycosaminoglycan scaffolds for tissue engineering, Biomaterials, 24, 4001–4009

Degasne I., Basne M.F., Demais V, Hure G., Lesourd M, Grollean B., Mercier L., Chappard D., 1999, Effects of roughness, fibronectin and vitronectin on attachment, spreading, and proliferation of human osteoblast-like cells (Saos-2) on titanium surfaces, Calcif. Tissue Int., 64, 499-507

Deligianni D.D., Katsala N.D., Koutsoukos P.G., Missirlis Y.F., 2001, Effect of surface roughness of hydroxyapatite on human bone marrow cell adhesion, proliferation, differentiation and detachment strength, Biomaterials, 22, 87-96

Dorotka R., Windberger U., Macfelda K., Bindreiter U., Toma C., Nehrer S., 2005, Repair of articular cartilage defects treated by microfracture and a three-dimensional collagen matrix, Biomaterials, 26, 3617-3629

Du C, Cui F.Z., Zhu X.D., de Groot K., 1998, Three-dimensional nano-HAp/collagen matrix loading with osteogenic cells in organ culture, J. Biomed. Mater. Res., 44, 407–415

Duan X., Sheardown H., 2006, Dendrimer crosslinked collagen as a corneal tissue engineering scaffold: Mechanical properties and corneal epithelial cell interactions, Biomaterials, *In press*

Dupps W. J., Wilson S.E., 2006, Biomechanics and wound healing in the cornea, Experimental Eye Research, *In press*

Eguchi H.,Hicks C.R.,Crawford G.J.,Tan D.T., Sutton G.R.,2004, Cataract surgery with the AlphaCor artificial cornea. J. Cataract Refract. Surg., 30, 1486-91

Falconnet D., Csucs G., Grandin H. M. , Textor M., 2006, Surface engineering approaches to micropattern surfaces for cell-based assays, Biomaterials, 27, 3044–3063

Fini M.E., 1999, Keratocyte and fibroblast phenotypes in the repairing cornea, Progress in Retinal and Eye Research, 18,5 29-551

Folch A., Jo B.H., Hurtado O., Beebe D.J., Toner M., 2000, Microfabricated elastomeric stencils for micropatterning cell cultures, J. Biomed. Mater. Res., 52, 346–353

Freyman T.M., Yannas I.V., Gibson L.J., 2001, Cellular materials as porous scaffolds for tissue engineering, Prog. In Materials Science, 46, 273-282

Fromstein J.D., Woodhouse K.A. , 2002, Elastomeric biodegradable polyurethane blends for soft tissue applications. J. Biomater. Sci. Polym. Ed., 13, 391–406

Funderburgh J., 2000, Keratan sulfate: Structure, biosythesis and function,Glycobiology, 10, 951-958

Funderburgh J.L., Funderburgh M.L., Mann M.M., Corpuz L., Roth M.R., 2003, Proteoglycan Expression during Transforming Growth Factor-induced Keratocyte-Myofibroblast Transdifferentiation, The Journal of Biological Chemistry, 276, 44173-44178

Funderburgh J.L., Mann M.M., Funderburgh M.L., 2003, Keratocyte Phenotype Mediates Proteoglycan Structure:A role for fibroblasts in corneal fibrosis, J. Biol. Chem., 46, 45629-45637

Galois L., Hutasse S., Cortial D., Rousseau C.F., Grossin L., Ronziere M., Herbage D., Freyria A., 2006, Bovine chondrocyte behaviour in three-dimensional type I collagen gel in terms of gel contraction,proliferation and gene expression, Biomaterials, 27, 79–90

Germain, L., Auger, F. A., Grandbois, E., Guignard, R., Giasson, M., Boisjoly, H. and Guerin, S. L., 1999, Reconstructed human cornea produced in vitro by tissue engineering, Pathobiology, 67, 140-147.

Germain L., Carrier P., Auger F. A. , Salesse C., Can we produce a human corneal equivalent by tissue engineering?, 2000 , Progress in Retinal and Eye Research, 5, 497-527

Gingras M., Paradis I., Berthod F., 2003, Nerve regeneration in a collagen–chitosan tissue-engineered skin transplanted on nude mice, Biomaterials, 24, 1653–1661

Gunatillake P.A, Adhikari R., 2003, Biodegradable synthetic polymers for tissue engineering, European Cells and Materials, 5, 1-16

Harada O., Kadota K., Yamamato T., 2001, Collagen-Based New Biomedicial Films: Synthesis, Property, and Cell Adhesion, Journal of Applied Polymer Science, Vol., 81, 2433–2438

Harris L.D., Kim B.S., Mooney D.S, 1998, Open pore biodegradable matrices formed with gas foaming, J. Biomed. Mater. Res., 42, 396–402

Harrison R.G., 1912, The cultivation of tissues in extraneous media as a method of morphogenetic study, Anat.Rec., 6, 181-193

Hasirci V, Vrana E., Zorlutuna P., Ndreu A., Yilgor P., Basmanav B., Aydin E., 2006, Nanobiomaterials; A review of the existing science and technology, and new approaches, Nanobiomaterials Special Edition of Journal of Biomaterials Science Polymer Edition, *In press*

Helary C., Foucault-Bertaud A., Godeau G., Coulomb B., Guille M.M.G., 2005, Fibroblast populated dense collagen matrices: cell migration, cell density and metalloproteinases expression, Biomaterials, 26, 1533-1543

Hicks C.R.,Chirila T.,Clayton A.B.,Fitton J.H ,Vijayasekaran S.,Dalton P.D., Lou X.,Platten S., Ziegelaar B., Hong Y., Crawford G.J., Constable I.J., 1998, Clinical

results of implantation of the Chirila keratoprosthesis in rabbits, Br J Ophthalmol, 8, 18-25

Hicks C. , Crawford G., Chirila T., Wien S., Vijayasekaran S., Lou X., Fitton J., Maley M., Clayton A., Dalton P., Platten S., Ziegelaar B., Hong Y., Russo A., Constable I. , 2000, Development and clinical assessment of an artificial cornea, Progress in Retinal and Eye Research Vol. 19, No. 2, 149-170

Hu X., Lui W., Cui L., Wang M.,Cao Y,,2005, Tissue Engineering of Nearly Transparent Corneal Stroma, Tissue Engineering , 11, 1710-1717

Huang Z., Hazlett L.D., 2003, Analysis of *Pseudomonas aeruginosa* corneal infection using an oligonucleotide microarray, Investigative Ophthalmology & Visual Science, 8, 3409-3416

Hutmacher D.W., 2000, Scaffolds in tissue engineering bone and cartilage,Biomaterials, 21, 2529-2543

Ignatius A., Blessing H., Liedert A., Schmidt C., Neidlinger-Wilke C., Kaspar D., Friemert B., Claes L., 2005, Tissue engineering of bone: effects of mechanical strain on osteoblastic cells in type I collagen matrices, Biomaterials, 26, 311-318

Itoh H., Aso Y., Furuse M., Noishiki Y., Miyata T., 2001, A honeycomb collagen carrier for cell culture as a tissue engineering scaffold, Artificial Organs, 25, 213-217

Jakus M.A., 1956, Studies on the cornea II: The fine structure of Descemet's membrane, J. Biophysic. And biochem. Cytol., 2, 243-255

Jester J.V,Moller-Pedersen T.,Huang J.,Sax C.M., Kay W.T.,1999,The cellular basis of corneal transparency: evidence for 'corneal crystallins', Journal of Cell Science, 112, 613-622

Jester J.V., Huang J., Fisher S., Spiekerman J., Chang J. H., Wright W.E., Shay J. W, 2003, Myofibroblast Differentiation of Normal Human Keratocytes and hTERT, Extended-Life Human Corneal Fibroblasts, Investigative ophthalmology and Visual Science, 5, 1850-1858

Ji Y., Ghosh K., Shu X.Z., Li B., Sokolov J.C., Prestwich G.D., Clark R.A.F., Rafailovich M.H., 2006, Electrospun three-dimensional hyaluronic acid nanofibrous scaffolds, Biomaterials, 27, 3782–3792

Jones I., Currie L. , Martin R., 2002, A guide to biological skin substitutes, British Journal of Plastic Surgery (2002), 55, 185–193

Karageorgiou V.,Kaplan D., 2005, Porosity of 3D biomaterial scaffolds and osteogenesis, Biomaterials, 26, 5474–5491

Kenar H., Köse G.T., Hasirci V., 2006, Tissue engineering of bone on micropatterned biodegradable polyester films, Biomaterials, 27, 885–895

Kim B.S., Mooney D.J., 1998, Development of biocompatible synthetic extracellular matrices for tissue engineering, Trends in Biotechnology,224-229

Kim W-J.,Rabinowitz Y.S., Meisler D.M., Wilson S.E. ,1999, Keratocyte apoptosis associated with Keratoconus, Experimental Eye Research, 5, 475-481

Klenkler B.J., Griffith M., Becerril C., West-Mays J.A., Sheardown H., 2005, EGF-grafted PDMS surfaces in artificial cornea applications, Biomaterials, 26, 7286–7296

Köse G.T, Ber S. , Korkusuz F.,Hasirci V.,2003, Poly(3-hydroxybutyric acid-co-3-hydroxyvaleric acid) based tissue engineering matrices, Journal of Materials Science:Materials in medicine, 14, 121-126

Köse G.T., Kenar H., Hasırcı N., Hasırcı V., 2003, Macroporous poly(3-hydroxybutyrate-co-3-hydroxyvalerate) matrices for bone tissue engineering, Biomaterials, 24, 1949–1958

Köse G.T, Korkusuz F., Özkul A., Soysal Y., Özdemir T., Yildiz C., Hasirci V., 2005, Tissue engineered cartilage on collagen and PHBV matrices, Biomaterials, 26, 5187–5197

Kubota A. , Nishida K. , Yamato M. , Yang J. , Kikuchi A., Okano T., Tano Y.,2006, Transplantable retinal pigment epithelial cell sheets for tissue engineering, Biomaterials, 27, 3639–3644

Kuroyanagi Y., Yamada N., Yamashita R., Uchinuma E., 2001, Tissue-engineered product: Allogeneic cultured dermal substitute composed of spongy collagen with fibroblasts, Artificial Organs, 25, 180-186

Lam M.T., Sim S., Zhu X.,Takayama S., 2006, The effect of continuous wavy micropatterns on silicone substrates on the alignment of skeletal muscle myoblasts and myotubes,Biomaterials, 27, 4340–4347

Lampin M., Warocquier-Clerout R., Legris C., Degrange M., Sigot-Liuzard M.F., 1997, Correlation between dubstratum roughness and wettability, cell adhesion, and cell migration, Journal of Biomedical Material Research, 36, 99-108

Langer R, Vacanti J.P. , 1993, Tissue engineering, Science, 260, 920-926.

Lavik E.,Langer R., 2004,Tissue engineering: current state and perspectives, Appl. Microbiol. Biotechnol., 65, 1–8

Lee C.H., Singla A., Lee Y., 2001, Biomedical applications of collagen, International Journal of Pharmaceutics, 221, 1-22

Lee C.R. , Grodzinsky A.J. , Spector M., 2001, The effects of cross-linking of collagen-glycosaminoglycan scaffolds on compressive stiffness, chondrocyte-mediated contraction, proliferation and biosynthesis, Biomaterials, 22, 3145–3154

Lee J.E., Kim K.E., Kwon I.C., Ahn H.J., Lee S., Cho H. Kim H.J., Seong S.C., Lee M.C., 2004, Effects of the controlled-released TGF-b1 from chitosan microspheres on chondrocytes cultured in a collagen/chitosan/ glycosaminoglycan scaffold, Biomaterials, 25, 4163–4173

Lee L.J., 2006, Polymer Nanoengineering for Biomedical Applications, Annals of Biomedical Engineering, 34, 75–88

Li C., Vepari C.,Jin H.J.,Kim H.J., Kaplan D., 2006, Electrospun silk-BMP-2 scaffolds for bone tissue engineering, Biomaterials, 27, 3115–3124

Li F. , Griffith M. , Li Z. , Tanodekaew S. , Sheardown H. , Hakim M.,Carlsson D.J., 2005, Recruitment of multiple cell lines by collagen-synthetic copolymer matrices in corneal regeneration, Biomaterials, 26, 3093-3104

Liu X., Won Y., Ma P.X., 2006, Porogen-induced surface modification of nano-fibrous poly(L-lactic acid) scaffolds for tissue engineering, Biomaterials, 27, 3980–3987

Liung Z., Huang A.Pflugfelder S.A., 1999, Evaluation of corneal thickness and topography in normal eyes using Orbscan corneal topography system, Br. J. Opthalmology, 83, 774-778

Lu L., Peter S.J., Lyman M.D., Lai H.L., Leite S.M., Tamada J.A., Vacanti J.P., Langer R., and Mikos A.G., 2000, In vitro degradation of porous poly(L-lactic acid) foams,Biomaterials, 21, 1595-1605

Lu Q.,Simionescu A., Vyavahare N., 2005, Novel capillary channel fiber scaffolds for guided tissue engineering, Acta Biomaterialia, 1, 607–614

Lu Y., Fukuda K, Li Q., Kumagai N., Nishida T., 2006, Role of nuclear factor-κB in interleukin-1-induced collagen degradation by corneal fibroblasts, Experimental Eye Research, 83, 560-568

Ma P.X., 2004, Scaffolds for tissue fabrication, Materials Today, 7, 30-40

Ma L., Gao C, Mao Z., Zhou J., Shen J., 2004, Biodegradability and cell-mediated contraction of porous collagen scaffolds: The effect of lysine as a novel crosslinking bridge, J. Biomed. Mater. Res., 71A, 334–342

Maquet V., Blacher S., Pirard R., Pirard J.-P., Vyakarnam M. N., Jerome R., 2003, Preparation of macroporous biodegradable poly(L-lactide*co*-ε-caprolactone) foams and characterization by mercury intrusion porosimetry, image analysis, and impedance spectroscopy, J. Biomed. Mater. Res., 66A, 199–213

Matsuzaka K.,Walboomers X.F., Yoshinari M., Inoue T., Jansen J.A., 2003, The attachment and growth behaviour of osteoblast-like cells on microtextured surfaces, Biomaterials, 24, 2711-2719

Maurice D.M., 1956, Structure and transparency of the cornea, Journal of Physio., 136, 263-286

Meek K.M., Leonard D.W,1993, Ultrastructure of the corneal stroma: a comparative study, Biophys. Journal, 64, 273-280

Meek K.M., Fullwood N.J., 2001, Corneal collagens: Corneal and scleral collagens—a microscopist's perspective, Micron, 32, 261-272

Mikos A.G., Bao Y., Cima L.G., Ingber D.E., Vacanti J.P., Langer R., 1993, Preparation of poly(glycolic acid) bonded fiber structures for cell attachment and transplantation, J. Biomed. Mater. Res., 27, 183-189

Moran J.M., Pazzano D., Bonassar L.J., 2003, Characterization of Polylactic Acid–Polyglycolic acid composites for cartilage tissue engineering, Tissue engineering, 9, 63-70

Müller F.A., Müller L., Hofmann I.,Greil P., Wenzel M.M.,Staudenmaier R., 2006, Cellulose-based scaffold materials for cartilage tissue engineering, Biomaterials, 27 , 3955–3963

Myllyharju J., Kivirikko K.I., 2001, Collagens and collagen-related diseases, Ann. Med., 33, 7-21

Ng K.W, Hutmacher D.W., 2006, Reduced contraction of skin equivalent engineered using cell sheets cultured in 3D matrices, Biomaterials, 27, 4591-4598

O'Brien F.J., Harley B.A., Yannas I.V., Gibson L.J., 2005, The effect of pore size on cel adhesion in collagen-GAG scaffolds, Biomaterials, 26, 433-441

Orwin E.J, Borene M.L., Hubel A., 2003,Biomechanical and optical characteristics of a Corneal stromal equivalent,Journal of Biomechanical Engineering, 125, 439-445

Orwin E.J, Hubel A, 2000, *In Vitro* Culture Characteristics of Corneal Epithelial, Endothelial, and Keratocyte cells in a Native Collagen Matrix, Tissue Engineering, 6, 307-319

Pancholi S., Tullo A., Khaliq A., Foreman D., Boulton M., 1999, The effects of growth factors and conditioned media on the proliferation of human corneal epithelial cells and keratocytes, Graefe's Arch. Clin. Exp. Ophthalmol., 236, 1-8

Park T.G., 2002, Perfusion culture of hepatocytes within galactose-derivatized biodegradable poly(lactide-*co*-glycolide) scaffolds prepared by gas foaming of effervescent salts, J. Biomed. Mater. Res., 59, 127–135

Pek Y.S.,Spector M., Yannas I.V., Gibson L.J., 2004, Degradation of a collagen–chondroitin-6-sulfate matrix by collagenase and by chondroitinase, Biomaterials, 25, 473-482

Pena J., Corrales T., Barba I.I., Doadrio A.L., Vallet-Regi M., 2006, Long term degradation of poly(3-caprolactone) films in biologically related fluids, Polymer Degradation and Stability , 91, 1424-1432

Pieper J.S., Oosterhof A., Dijkstra P.J. , Veerkamp J.H. , van Kuppevelt T.H., 1999, Preparation and characterization of porous crosslinked collagenous matrices containing bioavailable chondroitin sulphate,Biomaterials, 20, 847-858

Pieper J.S., van der Kraan P.M., Hafmans T., Kamp J., Buma P, van Susante J.L.C. , van den Berg W.B., Veerkamp J.H., van Kuppevelt T.H., 2002 ,Crosslinked type II collagen matrices: preparation, characterization, and potential for cartilage engineering, Biomaterials, 23, 3183–3192

Radisic M., Yang L.,Boublik J.,Cohen R.J.,Langer R., Freed L.E., Vunjak-Novakovic G., 2004, Medium perfusion enables engineering of compact and contractile cardiac tissue, Am. J. Physiol. Heart. Circ. Physiol., 286, 507–516

Rama P, Bonini S., Lambiase A, Golisano O., Osvaldo P., Paterna P, De Luca M., Pellegrini G., 2001, Autologous fibrin cultured limbal stem cells permanently restore the corneal surface of patients with total limbal stem cell deficiency, Transplantation, 72, 1478-1485

Ranucci C.S., Kumar A., Batra S.P., Moghe P.V., 2000, Control of hepatocyte function on collagen foams sizing matrix pores toward selective induction of 2-D and 3-D cellular morphogenesis, Biomaterials, 21, 783-793

Recknor J.B. , Sakaguchi D.S., Mallapragada S.K., 2006, Directed growth and selective differentiation of neural progenitor cells on micropatterned polymer substrates, Biomaterials, 27, 4098–4108

Ricci R.,Pecorella I., Ciardi A., Della Rocca C., Di Tondo U., Marchi V, 1992, Strampelli's osteo-odonto-keratoprosthesis. Clinical and histological long-term features of three prostheses, British Journal of Ophthalmology, 76, 232-234

Robert L. , Legais J.M. ,Robert A.M. , Renard G., 2001, Corneal collagens, Pathol. Biol., 49, 353-363

Rodrigues C.V.M., Serricella P., Linhares A.B.R., Guerdes R.M., Borojevic R., Rossi M.A., Duarte M.E.L., Farina M., 2003, Characterization of a bovine collagen–hydroxyapatite composite scaffold for bone tissue engineering, Biomaterials, 24, 4987–4997

Sachlos E., Czernuszka J.T. , 2003, Making tissue engineering scaffolds work: Review on the application of solid freeform fabrication technology to the production of tissue engineering scaffolds, European Cells and Materials, 5, 29-40

Schoof H., Apel J., Heschel I., Rau G. , 2001, Control of pore structure and size in freeze-dried collagen sponges, J. Biomed. Mater. Res. (Appl. Biomater.), 58, 352-357

Shieh S., Vacanti J. P., 2005, State of the art tissue engineering, Surgery, 1, 1-7

Stark Y., Suck K., Kasper C., Wieland M., van Griensven M., Scheper T., 2006, Application of collagen matrices for cartilage tissue engineering, Experimental and Toxicologic Pathology, 57, 305–311

Sumita Y., Honda M.J., Ohara T. , Tsuchiya S, Sagara H., Kagami H., Ueda M., 2006, Performance of collagen sponge as a 3-D scaffold for tooth-tissue engineering, Biomaterials , 27, 238–3248

Tezcaner A., Bugra K., Hasirci V., 2003, Retinal pigment epithelium cell culture on surface modified poly(hydroxybutyrate-co-hydroxyvalerate) thin films, Biomaterials, 24, 4573-4583

Tsai C., Hsu S., Cheng W., 2002, Effect of different solvents and crosslinkers on cytocompatibility of type II collagen scaffolds for chondrocyte seeding, Artificial organs, 26, 18-26

Tsang V.L., Bhatia S.N., 2004, Three-dimensional tissue fabrication, Advanced Drug Delivery Reviews, 56, 1635-1647

van Susante J.L.C. , Pieper J., Buma P.,van Kuppevelt T.H., van Beuningen H., van der Kraan P.M., Veerkamp J.H., van den Berg W.B., Veth R.P.E., 2001, Linkage of chondroitin-sulfate to type I collagen sca!olds stimulates the bioactivity of seeded chondrocytes in vitro, Biomaterials , 22, 2359-2369

Walboomers F.X, Jansen J.A., 2001, Cell and tissue behaviour on micro-grooved surfaces, Odontology, 89, 2-11

Wan Y.,Wang Y.,Liu Z., Qu X, Han B., Bei J., Wang S., 2004, Adhesion and proliferation of OCT-1 osteoblast-like cells on micro and nano scale topography structure poly(L-lactide), Biomaterials, 26, 4453-4459

Wei H.J. , Liang H., Lee M., Huang Y., Chang Y.,Sung H., 2005, Construction of varying porous structures in acellular bovine pericardia as a tissue-engineering extracellular matrix, Biomaterials, 26, 1905–1913

West-Mays J. A., Dwivedi D. J., 2006 , The keratocyte: Corneal stromal cell with variable repair phenotypes, The International Journal of Biochemistry & Cell Biology, *In press*

Wiesmann H.P. , Nazer N. , Klatt C., Szuwart T., Meyer U., 2003, Bone tissue engineering by primary osteoblast-like cells in a monolayer system and 3-Dimensional collagen gel, Journal of Oral and Maxillofacial Surgery, 61, 1455-1462

Wilson S.E., Kim W.J., 1998, Keratocyte Apoptosis: Implications on corneal wound healing, tissue organization and disease, Investigative Ophthalmology & Visual Science, 2, 220-226

Wilson S.E., Pedroza L. , Beuerman R., Hill J.M., 1997, Herpes Simplex virus type-1 infection of corneal epithelial cells induces apoptosis of the underlying keratocytes, Experimental Eye Research, 5, 775-779

Yamauchi K., Takeuchi N., Kurimoto A., Tanabe T., 2001, Films of collagen crosslinked by S-S bonds: preparation and characterization, Biomaterials, 22, 855-863

Yannas I.V., Lee E., Orgill D.P., Skrabut E.M., Murphy G.F., 1989, Synthesis and characterization of a model extracellular matix that induces partial regeneration of adult mammalian skin, Natl. Acad. Sci. USA, 86, 933-937

Yao C., Roderfeld M, Rath T., Roeb E., Bernhagen J., Steffens G., 2006, The impact of proteinase-induced matrix degradation on the release of VEGF from heparinized collagen matrices, Biomaterials, 27, 1608–1616

Yap F.L., Zhang Y., 2006, Protein and cell micropatterning and its integration with micro/nanoparticles assembly, Biosensors and Bioelectronics, *In press*

Yaylaoglu M.B., Yıldız C., Korkusuz F., Hasirci V., 1999, A novel osteochondral implant, Biomaterials, 20, 1513-1520

Yunoki S, Nagai N., Suzuki T., Munekata M., 2004, Novel biomaterial from reinforced salmon collagen gel prepared by fibril formation and cross-linking, Journal of Bioscience and Bioengineering, 98, 40-47

Zhong S.P., Teo W.E., Zhu X., Beuerman R., Ramakrishna S., Yung L.Y.L. , 2006, Development of a novel collagen–GAG nanofibrous scaffold via electrospinning, Materials Science and Engineering C, *In press*

APPENDICES

APPENDIX A

MTS Calibration curve

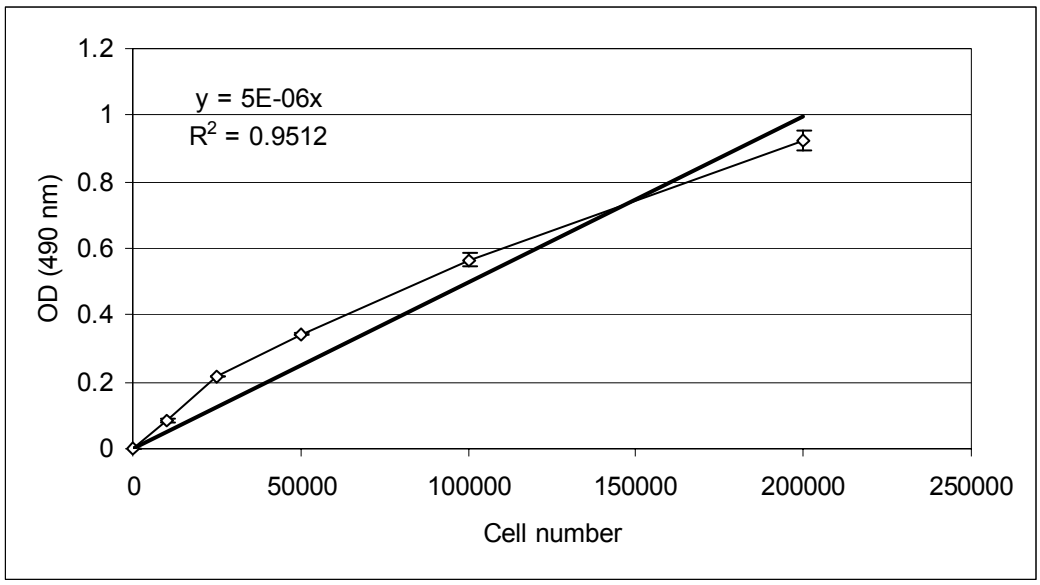

Figure A.1. Calibration curve of MTS assay for keratocytes

Medium composition for the assay: 10 ml of %10 MTS solution contains 9 ml DMEM Low glucose medium 952 µl MTS and 48 µl PMS.